AD-A055 924 COLORADO STATE UNIV FORT COLLINS DEPT OF ELECTRICAL --ETC F/G 9/4
MODULO-2 PI PHASE SEQUENCE ESTIMATION.(U)
FEB 78 L L SCHARF, D D COX, C J MASRELIEZ N00014-75-C-0518
UNCLASSIFIED TR-27(ONR) NL

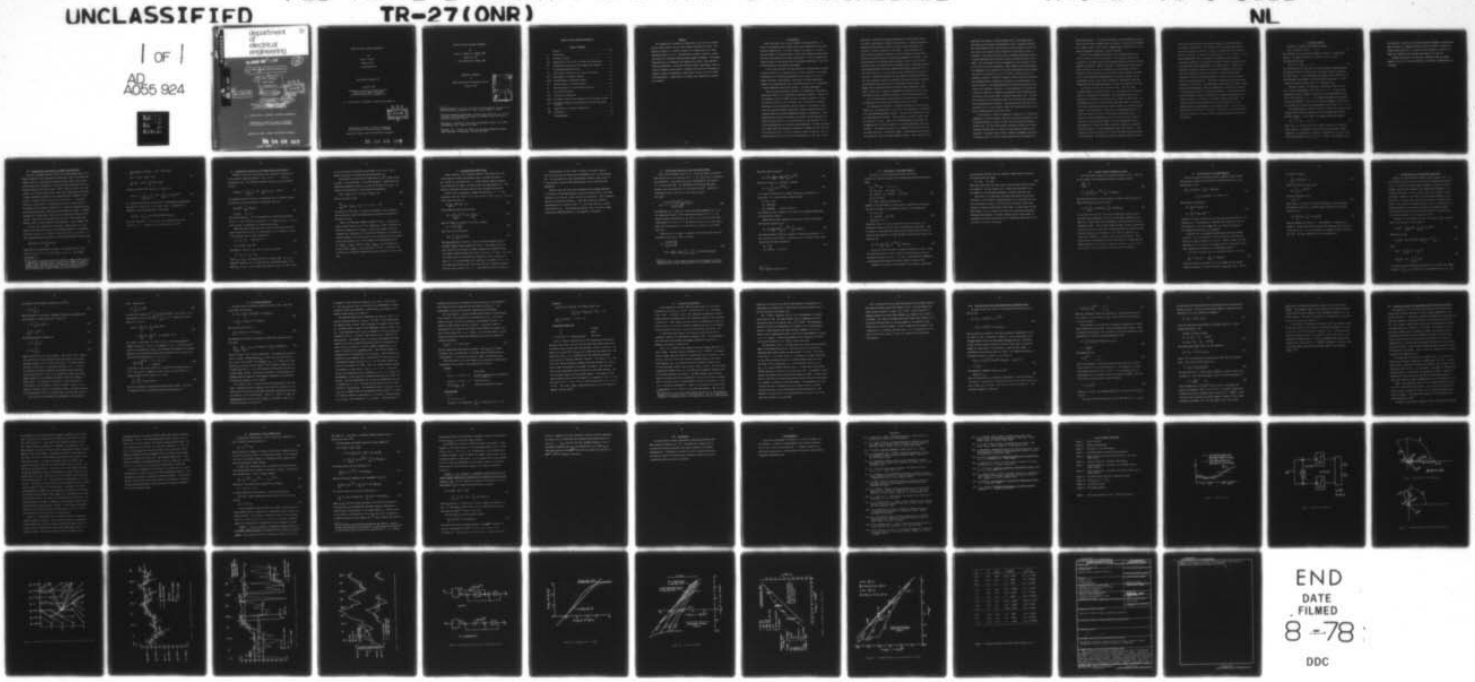

END
DATE FILMED
8-78
DDC

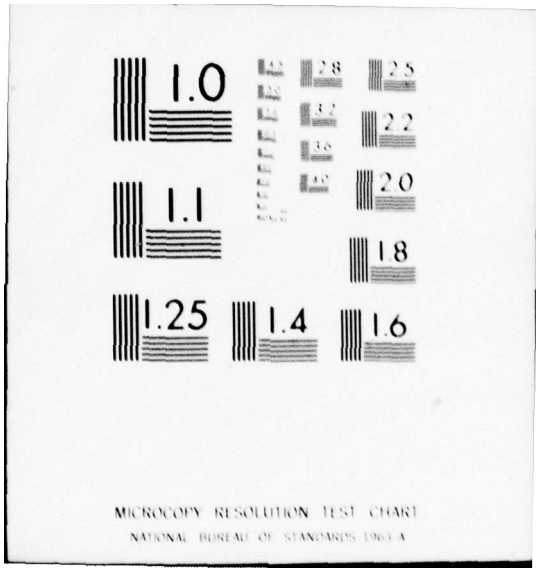
1.0
1.1
1.25
1.4
1.6
2.8
2.5
3.2
2.2
3.6
2.0
4.0
1.8
MICROCOPY RESOLUTION TEST CHART
NATIONAL BUREAU OF STANDARDS 1963-A

department of electrical engineering

(12)

(6) Modulo-2π Phase Sequence Estimation

by

(10) Louis L. Scharf,
Dennis D. Cox
C. Johan Masreliez

(14) TR-27(ONR)

(9) Technical Report, 27

(11) February 1978

(12) 66p.

Prepared for the Office of Naval Research
under Contract N00014-75-C-0518
with joint sponsorship of NAVALEX 320

L. L. Scharf and M. M. Siddiqui, Principal Investigators

Modulo-2π Phase Sequence Estimation

by

Louis L. Scharf

Dennis D. Cox

C. Johan Masreliez

ONR Technical Report #27

February 1978

Prepared for the Office of Naval Research
under Contract N00014-75-C-0518
with joint sponsorship of NAVALEX 320

L. L. Scharf and M. M. Siddiqui, Principal Investigators

Modulo-2π Phase Sequence Estimation

by

Louis L. Scharf[1], Sr. Member IEEE

Dennis D. Cox[2]

C. Johan Masreliez[3], Member IEEE

Manuscript Submitted

to

IEEE Transactions on Information Theory

February 1978

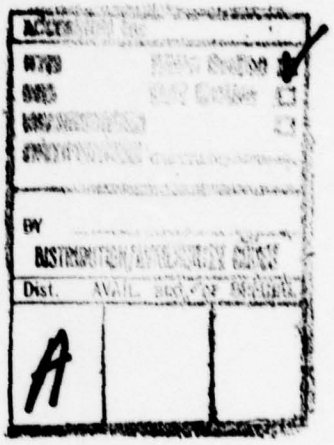

This work supported in part by the Office of Naval Research, Statistics and Probability Branch, Arlington, VA, under Contract N00014-75-C-0518.

[1]Electrical Engineering Department, Colorado State University, Ft. Collins, CO, 80523, and Laboratoire des Signaux et Systèmes, Plateau du Moulon, 91190 Gif-sur-Yvette, France.

[2]Department of Mathematics, University of Washington, Seattle, WA, 98195, and Honeywell, Inc., Seattle, WA, 98107.

[3]Honeywell, Inc., Seattle, WA, 98107, and Electrical Engineering Department, University of Washington, Seattle, WA, 98195.

Modulo-2π Phase Sequence Estimation

Table of Contents

Abstract

The probabilistic evolution of random walk on the circle is studied and the results used to derive a MAP sequence estimator for phase. The sequence estimator is a Viterbi tracker for tracking phase on a finite-dimensional grid in $[-\pi,\pi)$. The algorithm is shown to provide a convenient method for obtaining fixed-lag phase sequence estimates. Performance characteristics are presented and compared with several other nonlinear filtering algorithms. The results indicate superior performance over the range of parameter values usually considered and excellent performance in parameter ranges corresponding to high signal-to-noise ratio and rapidly fluctuating phase. Applications to coherent data communication systems are outlined.

I. Introduction

Phase tracking is the classic nonlinear filtering problem. It arises in narrowband analog communication, data transmission, and spread spectrum communication. As usually stated, the problem is to obtain a causal estimate of the phase based on noisy, phase-modulated observations. The best known solutions are phase locked loops. In data transmission a fixed-lag delay in the estimate may be acceptable, especially if the delay offers significant performance improvement.

In any truly nonlinear filtering approach to optimum phase tracking, the basic problem is to propagate the *a posteriori* density of the phase, conditioned on an increasing measurement record, much as is done in Kalman filtering. Unfortunately, there exist no finite-dimensional schemes for propagating the exact conditional density or for propagating a finite-dimensional sufficient statistic. One must approximate.

There are many approaches available for propagating an approximate conditional density or an approximate sufficient statistic. One may use the maximum *a posteriori* (MAP) interval estimation equations of Lehan and Parks [1] and Youla [2] to obtain a set of differential equations satisfied by the noncausal MAP interval estimate. The boundary conditions are two-point boundary conditions. Causal approximations may be obtained using the invariant-imbedding technique of Bellman [3]. This approach has been used by Detchmendy and Sridhar [4] and Baggeroer [5]. As Van Trees [6] points out in his discussion of this approach, the required approximations are linearizing approximations. Another alternative is to begin with the differential equations of Kushner [7] that describe the evolution of the *a posteriori* density of Markov processes. The resulting equations can only be solved approximately in the case of phase

modulation. Snyder [8] has used this approach to obtain phase locked loop (PLL) type trackers. Willsky [9] has used it to obtain propagation equations for the Fourier series coefficients that characterize the periodic *a posteriori* density for the phase. A third approach is to pose the phase estimation problem as a state estimation problem involving state variables that are functionally dependent on the phase. These state equations are differentiated according to the Ito rule to obtain dynamical state equations with state-dependent noise. Using this approach Bucy and Mallinckrodt [10] have obtained differential equations for the conditional density of the state and for the conditional expectation of the state. Taking this approach one step further, Gustafson and Speyer [11] have obtained an explicit realizable filtering structure by imposing the constraint that the filter be of the Kalman filter variety. The Kalman gain is optimized and the resulting "linear quadrature" filter (LQF), a fancy PLL, is shown to outperform the classical PLL and to perform almost as well as Willsky's Fourier coefficient filter (FCF) [9].

All of the approaches outlined above are continuous-time in nature, although many of them have been simulated in discrete-time.

The fundamental difficulty of nonlinear filtering in discrete-time remains one of propagating an *a posteriori* filtering density, conditioned on an increasing measurement sequence. The governing equations are the so-called Bayesian recursions. These equations are easy to write down but difficult to solve. There is no finite-dimensional algorithm for propagating the *a posteriori* density or a finite-dimensional sufficient statistic. The simplest approach is to assume the *a posteriori* density is normal and then to recursively compute a conditional mean and covariance along the lines of extended Kalman filtering. Kelly and Gupta [12]

have used this approach to obtain digital PLLs. More sophisticated approaches involve sharper approximations to the *a posteriori* density. Bucy and Mallinckrodt [10] have derived an up-date formula for the discrete-time cyclic density that describes the *a posteriori* density of the phase. This formula has been used to propagate probability mass on a finite-dimensional grid and obtain their so-called point-mass filter (PMF). Bucy and Youssef [13] have expanded the cyclic density of [10] in a Fourier series and propagated a finite number of the coefficients. The advantage of this method over the point mass method is that computation times are reduced by a factor of 8 [13]. Willsky [9] has also expanded a periodic *a posteriori* density in Fourier series coefficients and propagated these coefficients according to a multiplicative rule that is related to the Chapman-Kolmogorov convolution that must be performed in the Bayesian recursions. A third approach is to expand the *a posteriori* density of in-phase and quadrature state variables using the Gaussian sum formula (GSF) of Sorenson and Alspach [14]. The mean and covariance of the individual terms in the sum are then propagated as new measurements are obtained. This approach has been used by Tam and Moore [15] to obtain a phase tracker that performs about as well as Bucy and Mallinckrodt's point mass filter.

In this paper we propose an approach to phase *sequence* estimation (emphasis on the word sequence) that has its logical antecedents in the filtering philosophy of Youla [2] and the data decoding philosophy of Viterbi [16]. We pose a MAP sequence estimation problem that leads to nonlinear MAP equations not unlike the continuous-time MAP interval equations. Fortunately there exists a dynamic programming algorithm to efficiently solve for survivor phase sequences that approximate the

desired MAP sequence. The algorithm provides a handy mechanism for generating fixed-lag phase estimates that are superior to other known estimates. As is common in most of the current communications literature we call our dynamic programming algorithm a Viterbi algorithm.

Cahn [17] has suggested that phase may be tracked with delay in order to extend the so-called threshold. He proposes a Viterbi-like algorithm for tracking carrier phase sequences whose realizations satisfy dynamics constraints. There is certainly a philosophical link between Cahn's work and ours, but the approaches are really quite different. Ungerboeck [18] has proposed an algorithm for phase tracking that makes use of a delta-modulation approximation to the phase sequence and an approximate version of the Viterbi algorithm. Ungerboeck's modelling assumptions and algorithm development are also very different from ours.

An outline for this paper goes as follows. The basic phase tracking problem is posed in Section II. In Sections III-V a tractable model for random phase is developed. The development begins with a discussion of random walk on the circle as a model for phase noise. An approximating process is then specified that makes Markov transitions at periodic sampling instants and remains constant on intervals between samples. The probabilistic evolution of the approximating process is completely characterized by a folded normal conditional density. In Section VI these approximations are used to write the joint density function of the data and the phase as a finite-dimensional density. The sequence of envelope and phase statistics computed on contiguous intervals arises as a finite-dimensional sufficient statistic. These results are used in Section VII to restate the phase tracking problem in discrete-time. The MAP phase sequence estimation problem is posed

in Section VIII and several interesting properties of the MAP sequence are derived in Section IX. The solution for the constant phase acquisition case is derived in Section X, where it is shown that the estimator is modulo-2π unbiased. In Section XI the phase space $[-\pi,\pi)$ is discretized to a finite-dimensional grid, a path-metric is identified, and a Viterbi algorithm is derived to efficiently keep track of survivor sequences that can potentially become approximants to the MAP sequence. Fixed-lag (or fixed depth constant) versions of the Viterbi algorithm for obtaining fixed lag estimates of phase are discussed. The envelope and phase statistics, and the folded normal density of Section IV, enter the path metric in an interesting way. Illustrative simulations are presented and annotated in Section XII. The performance characteristics of phase locked loops and related Kalman filters are summarized in Section XIII and used to bound the performance of random phase trackers. In Section XIV Monte-Carlo performance results are presented and compared with published performance results for a variety of nonlinear filtering algorithms. The results show the Viterbi algorithm to be clearly superior to other algorithms both in performance *and* computation speed for applications in which moderate delays may be tolerated. Applications to coherent communication are outlined in Section XV and concluding remarks are advanced in Section XVI.

II. The Basic Problem

Consider the randomly phase modulated signal

$$X(t) = \cos[2\pi f_0 t + \Phi(t)] \quad , \quad t \geq 0 \tag{1}$$

The frequency f_0 is the carrier frequency and $\Phi(t)$ is a random phase process. The signal is observed in additive noise to produce the observation process

$$Z(t) = X(t) + N(t) \quad , \quad t \geq 0 \tag{2}$$

Our convention will be that upper case letters denote random processes and random variables, and that lower case letters denote realizations of these objects. In our subsequent development we will assume $N(t)$ is white Gaussian noise (WGN) of two-sided spectrum level $N_0/2$. By this convention we mean the noise power in a 1 Hz band is N_0.

The basic problem is to estimate a realization of $\Phi(t)$, call it $\phi(t)$, from the measurement record $\{z(s), 0 \leq s < t\}$. Of course this measurement record is simply a realization of the measurement process $Z(s)$ on the interval $0 \leq s < t$. The problem statement may be relaxed to allow the estimate of $\phi(t)$ to be a fixed-lag estimate, in which case the estimate may be based on the measurement record $\{z(s), 0 \leq s < t + \tau\}$.

The approximations of Sections III-V will permit us to replace this continuous-time problem statement with the following discrete-time problem statement. Let Z_k denote the complex observation sequence

$$Z_k = e^{j\Phi_k} + N_k \quad , \quad k = 1,2,\ldots \tag{3}$$

where $\{\Phi_k\}$ is a discrete-time phase sequence and $\{N_k\}$ is an additive noise sequence of independent identically distributed normal random variables. The problem is to estimate a realization of Φ_k, call it ϕ_k, from the measurement record $\{z_\ell, \ell=1,2,\ldots,k+k_0\}$. The parameter k_0 is

the fixed lag. Note that in this discrete-time statement the problem has been converted to a baseband problem in which the carrier frequency no longer enters explicitly. In Section VII we establish a connection between the continuous- and discrete-time models of (1) and (3).

We make the obvious, but important, observation that the signal models of (1) and (3) are both invariant to modulo-2π transformations on the phase.

III. Random Walk on the Circle as a Model for Phase Noise

The first, seemingly natural, choice for a random phase model is the Wiener process W(t) with incremental variance σ_0^2. This is the model most commonly used as a random phase acquisition model. Most of the results in this paper may be obtained in a formal way using this phase model, but certain technical difficulties arise. First, there is no stationary distribution in this model and, second, there is no rigorous way of defining a unique conditional probability for transitions from a modulo-2π value of $\phi(t)$ to another modulo-2π value at a later time $t + \tau$. The latter difficulty is particularly troublesome as one of the crucial parts of our modulo-2π phase sequence estimator is a transition probability matrix that characterizes phase transitions between modulo-2π values. By modeling phase as a random walk on the circle we avoid these technical difficulties. Other authors have noted that the circle is the appropriate domain on which to study modulo-2π type sequences. See for example [9].

Let $\Phi(t)$ be a random walk on the circle, taking values in $[-\pi,\pi)$. Denote by the function $p(\phi_t/\phi_s)$ the conditional density of a transition from the value $\Phi(s) = \phi_s$ at time s to the value $\Phi(t) = \phi_t$ at time $t \geq s$. This conditional density satisfies the partial differential equation [19]

$$\frac{\partial}{\partial t} p(\phi_t/\phi_s) = \frac{1}{2} \sigma_0^2 \frac{\partial^2}{\partial \phi_t^2} p(\phi_t/\phi_s) \tag{4}$$

where σ_0^2 is the infinitessimal variance. This equation holds in the strip $-\pi \leq \phi_t \leq \pi$, $t > s$, for any fixed $-\pi \leq \phi_s \leq \pi$. The boundary conditions[1] are

[1] We are using the convention that $\Phi(t)$ denotes a random variable and ϕ_t a realization. When the context is clear, and no danger of confusion exists, we will sometimes make no distinction in notation between a random variable and its realizations. The same cautionary note holds for the discrete-time random variables Φ_k and the realizations ϕ_k.

$$\lim_{t\to s} p(\phi_t/\phi_s) = \delta(\phi_t-\phi_s) \quad ; \ \delta(\cdot) : \text{Dirac delta}$$

$$p(\phi_t = -\pi/\phi_s) = p(\phi_t = \pi/\phi_s) \tag{5}$$

$$\frac{\partial}{\partial\phi_t} p(\phi_t = -\pi/\phi_s) = \frac{\partial}{\partial\phi_t} p(\phi_t = \pi/\phi_s)$$

A Laplace transform type solution for $p(\phi_t/\phi_s)$ is

$$p(\phi_t/\phi_s) = \frac{1}{\sqrt{2\pi\sigma_0^2(t-s)}} \sum_{n=-\infty}^{\infty} \exp\{-\frac{1}{2\sigma_0^2(t-s)} (\phi_t-\phi_s-n2\pi)^2\} \tag{6}$$

It is easily seen that the process $\Phi(t)$ is conditionally approximately $N(\phi_s,\sigma_0^2(t-s))$, given $\Phi(s) = \phi_s$ for small $(t-s)$. An eigenfunction expansion of the following form is also useful:

$$p(\phi_t/\phi_s) = \frac{1}{2\pi} \sum_{n=-\infty}^{\infty} \exp(-n^2\sigma_0^2 t/2)\exp(in\ (\phi_t-\phi_s)) \tag{7}$$

From this expression it is clear that $\Phi(t)$ becomes uniformly distributed as $t \to \infty$. Equation (7) has also been noted in [9].

IV. Probabilistic Evolution of the Sampled-Data Phase Sequence

Consider the discrete-time sequence $\{\Phi_k\}$ obtained by sampling $\Phi(t)$ at the periodic sampling instants $t = kT$, $k = 0,1,\ldots$. Call ϕ_k a realization of Φ_k. The transition density from ϕ_{k-1} to ϕ_k is obtained from (6):

$$p(\phi_k/\phi_{k-1}) = \frac{1}{\sqrt{2\pi\sigma_o^2 T}} \sum_{n=-\infty}^{\infty} \exp\{-\frac{1}{2\sigma_o^2 T}(\phi_k - \phi_{k-1} - n2\pi)^2\} \tag{8}$$

By the Markov property of $\Phi(t)$ it follows that $\{\Phi_k\}$ is a Markov sequence for which the joint distribution of $\{\Phi_k\}_1^K$ may be written

$$\begin{aligned} p_K(\{\phi_k\}_1^K) &= \prod_{k=1}^{K} p(\phi_k/\phi_{k-1}) \\ p(\phi_1/\phi_0) &: U[-\pi,\pi) \end{aligned} \tag{9}$$

The notation $p(\phi_1/\phi_0) : U[-\pi,\pi)$ indicates Φ_1 is uniformly distributed on $[-\pi,\pi)$. Other choices are admissable: for example $p(\phi_1/\phi_0) = \delta(\phi_1-\phi_0)$ with ϕ_0 known, corresponding to a known initial phase.

Neglecting some sticky questions of rigor one may obtain the same discrete-time model for $\{\Phi_k\}$ by considering Φ_k to be a modulo-2π version of the following discrete-time random walk:

$$\begin{aligned} \Theta_k &= \Theta_{k-1} + W_k \quad ; \quad W_k \perp\!\!\!\perp W_\ell \;\forall\, k \neq \ell \\ W_k &: N(0,\sigma_W^2) \; ; \; \sigma_W^2 = \sigma_o^2 T \end{aligned} \tag{10}$$

The modulo-2π version of Θ_k, call it $\bar{\Theta}_k$, may be written

$$\bar{\Theta}_k = \bar{\bar{\Theta}}_k \; ; \; \bar{\Theta}_k = \bar{\Theta}_{k-1} + W_k \tag{11}$$

Given $\bar{\Theta}_{k-1} = \bar{\theta}_{k-1}$, the random variable $\bar{\Theta}_k$ is $N(\bar{\theta}_{k-1},\sigma_W^2)$. As $\bar{\Theta}_k$ is a modulo-2π version of $\bar{\Theta}_k$ it follows that the conditional density of $\bar{\Theta}_k$, given $\bar{\Theta}_{k-1} = \bar{\theta}_{k-1}$, is the folded normal density of (8). For this reason

we will often call the discrete-time process on the circle, $\{\phi_k\}$, a modulo-2π version of the discrete-time random walk $\{\theta_k\}$.

In Section XI we discretize the phase space $[-\pi,\pi)$ to phase values ξ_m, m=0,..., M-1 with M odd. It is then necessary to characterize the transition probability from ξ_ℓ to ξ_m for all M^2 pairs of (ξ_ℓ,ξ_m). We choose for our definition of this transition probability

$$\bar{p}(\phi_k = \xi_m/\phi_{k-1} = \xi_\ell) = b_\ell \, p(\phi_k = \xi_m/\phi_{k-1} = \xi_\ell) \tag{12}$$

with b_ℓ selected so that

$$\sum_{m=0}^{M-1} \bar{p}(\phi_k = \xi_m/\phi_{k-1} = \xi_\ell) = 1, \; \ell = 0,1,\ldots, M-1 \tag{13}$$

The sum on n in (8) must, of course, be truncated. This truncation may be selected to give the desired accuracy before the algorithm of Section XI is run.

There is an important symmetry property of (12). If the ξ_ℓ are equally spaced points on $[-\pi,\pi)$, for example $\xi_\ell = \ell 2\pi/M - (M-1)\pi/M$, the function $\bar{p}$ depends only on $|\xi_m-\xi_\ell|$. Thus if the values of (12) are organized into an MxM matrix of transition probabilties, the matrix has Toeplitz symmetry with each successive row a one-position cyclic permutation of the previous row. We may compute the M-dimensional vector $\bar{Q} = (\bar{q}_0,\bar{q}_1,\ldots,\bar{q}_{M-1})$, with $\bar{q}_n = \bar{p}(\phi_k = \xi_0/\phi_{k-1} = \xi_n)$ and obtain any value of $\bar{p}(\phi_k = \xi_m/\phi_{k-1} = \xi_\ell)$ as $\bar{q}_n$ with $n = |m-\ell|$. In this way only an M-vector of transition probabilities need be stored for cyclic reading.

V. An Approximating ZOH Process

Shown in Figure 1 is a conceptual sketch of the process $\Phi(t)$ and a zero-order hold (ZOH) approximation that is constant and equal to $\Phi_k = \Phi(t=kT)$ on the interval $kT \leq t < (k+1)T$ between sampling instants. It is noted that for small T the ZOH process will approximate $\Phi(t)$. This heuristic observation is made precise by the following calculations.

Without loss of generality consider the interval $0 \leq t < T$. The probability that $\Phi(t)$ differs from a given value of $\Phi(0) = \phi_0$ by δ or more on this T second interval is

$$P[\{\sup_{0\leq s<T} |\Phi(s)-\phi_0| \geq \delta\}] \tag{14}$$

This probability may be written [20]

$$P[\cdot] = \frac{2\delta}{\sqrt{2\pi\sigma_0^2}} \int_0^T t^{-3/2} \exp(-\frac{\delta^2}{2\sigma_0^2 t})dt \tag{15}$$

Make the change of variable $x = \delta t^{-\frac{1}{2}}/\sigma_0$ to obtain

$$P[\cdot] = 4Q(\delta/\sqrt{\sigma_0^2 T}) \tag{16}$$

where Q(x) is the Q-function:

$$Q(x) = \int_x^\infty \frac{1}{\sqrt{2\pi}} \exp(-\delta^2)d\delta \tag{17}$$

The interpretation is that $P[\cdot]$ is four times the probability that a $N(0,\sigma_0^2 T)$ random variable exceeds the value δ. The result of (16) is twice the result one obtains by simply computing the probability that the terminal random variable $\Phi(T)$ differs from ϕ_0 by δ or more. The factor of 2 takes care of trajectories that exceed the $\pm\delta$-band around ϕ_0 for some $0 \leq t < T$ and then wander back toward ϕ_0 to be within $\pm\delta$ at $t = T$. The reflection principle says every such path has a reflection counterpart that stays outside $\pm\delta$ at $t = T$. This takes care of the factor of 2.

The importance of (16) is that it allows us to select triples $(P[\cdot],\delta,T)$ such that the ZOH process approximates $\Phi(t)$ in a well-defined way. For processes with large infinitessimal variance, small values of T are required to keep the ZOH approximation close to $\Phi(t)$ with high probability.

Finally, note that the results obtained here go through unchanged if we select our ZOH approximation to match the process $\Phi(t)$ at the right end-point of an interval, rather than the left end-point. Such an approximation is illustrated in Figure 1. With this choice the process is approximated on the interval $(k-1)T < t \leq kT$ by the value $\Phi_k = \Phi(t=kT)$, rather than by Φ_{k-1}. This simplifies notation a bit, so we will assume this kind of ZOH approximation in the remainder of the paper.

VI. Joint Density Function of the Data and the Phase

Recall the measurement model of (1). Let $Z(t;k)$ denote the measurement process $Z(t)$ on the interval $(k-1) < t \leq kT$, and $z(t;k)$ a corresponding realization. The process $Z(t)$ may be represented on the interval $0 < t \leq KT$ as $\{Z(t;k)\}_1^K$. Let $\{\phi_k\}_1^K$ denote the discrete-time phase sequence that characterizes $\Phi(t)$ on the same interval[2]. Consider the following likelihood function for $\{Z(t;k)\}_1^K$ and $\{\phi_k\}_1^K$:

and $\{\phi_k\}_1^K$:

$$D_K = \frac{f_1\{z(t;k)\}_1^K/\{\phi_k\}_1^K) \prod_{k=1}^{K} p(\phi_k/\phi_{k-1})}{f_0(\{z(t;k)\}_1^K)} \tag{18}$$

The densities $f_1(\cdot/\cdot)$ and $f_0(\cdot/\cdot)$ have only formal meaning: $f_1(\cdot/\cdot)$ is the conditional density for the observation process $Z(t)$, $0 < t \leq KT$, given the phase realization $\Phi_k = \phi_k$, $k=1,2,\ldots,K$; $f_0(\cdot/\cdot)$ is the conditional density for $Z(t)$, $0 < t \leq KT$, given only noise in the measurement. From this interpretation it is clear that $f_1(\cdot/\cdot)/f_0(\cdot/\cdot)$ is a likelihood ratio.

Using any one of a number of standard tricks [21] we may write the likelihood ratio part of (18) as follows:

$$\begin{aligned} L_K &= \frac{f_1(\{z(t;k)\}_1^K)}{f_0(\{z(t;k)\}_1^K)} \\ &= \exp\{-\frac{K}{2N_0/T} + \frac{2}{2N_0/T} \sum_{k=1}^{K} \frac{2}{T} \int_{(k-1)T}^{kT} z(t;k)\cos(2\pi f_0 t+\phi_k)dt\} \end{aligned} \tag{19}$$

---

[2] Recall the sense of the characterization: $\Phi(t)$ is assumed to be well-modelled by the constant value $\Phi_k=\Phi(t=kT)$ on the interval $(k-1)T<t\leq kT$.

This result may be written[3]

$$L_K = \exp\{-\frac{K}{2N_0/T} + \frac{2}{2N_0/T}\,\mathrm{Re}\sum_{k=1}^{K} z_k e^{-j\phi_k}\} \tag{20}$$

where the variable z_k is defined as follows:

$$z_k = \frac{2}{T}\int_{(k-1)T}^{kT} z(t)e^{-j2\pi f_0 t}\,dt \tag{21}$$

It is easily verified that the random variable Z_k, of which z_k is a realization, is a complex normal random variable:

$$\begin{aligned} Z_k &= U_k + j\,V_k \\ U_k &: N(0,N_0/T) \\ V_k &: N(0,N_0/T) \qquad U_k \perp\!\!\!\perp V_k \quad \Psi(k,\ell) \end{aligned} \tag{22}$$

The variable z_k may be viewed as the output of a quadrature demodulator as illustrated in Figure 2.

Neglecting the data independent term of L_K in (18), we may write the likelihood function D_K as

$$D_K = \exp\{\frac{1}{2N_0/T}\,2\mathrm{Re}\sum_{k=1}^{K} z_k e^{-j\phi_k}\}\prod_{k=1}^{K} p(\phi_k/\phi_{k-1}) \tag{23}$$

The complex sequence $\{Z_k\}_1^K$ is a sequence of sufficient statistics. It will be useful in the sequel to interpret results in terms of the following envelope and phase statistics:

$$\begin{aligned} C_k &= |Z_k| \\ \Psi_k &= \arg Z_k \quad ; \quad \Psi_k \in [-\pi,\pi) \end{aligned} \tag{24}$$

---

[3] Re(·) denotes "real part of."

VII. Restatement of the Basic Problem

The result of (23) is identical with the likelihood function for $\{Z_k\}_1^K$ and $\{\Phi_k\}_1^K$ in the following discrete-time observation model:

$$
\begin{aligned}
&Z_k = e^{j\Phi_k} + N_k \quad , \quad k = 1,2,\ldots \\
&N_k = U_k + jV_k \quad , \quad N_k \perp\!\!\!\perp N_\ell \;\forall\; k \neq \ell \\
&U_k : N(0,\sigma_n^2) \;,\; V_k : N(0,\sigma_n^2) \quad ; \quad \sigma_n^2 = N_0/T \\
&U_k \perp\!\!\!\perp V_\ell \;\forall\; (k,\ell) \\
&\Phi_k : \text{phase sequence defined by (8)}
\end{aligned}
\tag{25}
$$

Subject to the disclaimers of rigor stated in Section IV, the process $\{\Phi_k\}$ may be thought of as a modulo-2π version of the random walk

$$
\begin{aligned}
&\Theta_k = \Theta_{k-1} + W_k \\
&W_k : N(0,\sigma_W^2) \quad ; \quad \sigma_W^2 = \sigma_0^2 T \\
&W_k \perp\!\!\!\perp W_\ell \;\forall\; k \neq \ell
\end{aligned}
\tag{26}
$$

This means, under the ZOH approximations stated in Section V, the observation models of (1) and (25) are statistically equivalent. Thus we replace a continuous-time problem with a discrete-time one and consider the joint density of $\{Z_k\}_1^K$ and $\{\Phi_k\}_1^K$, written now in terms of the parameter σ_n^2:

$$
D_K = \exp\left\{\frac{1}{2\sigma_n^2}\, 2\mathrm{Re} \sum_{k=1}^{K} z_k e^{-j\phi_k}\right\} \prod_{k=1}^{K} p(\phi_k/\phi_{k-1}) \tag{27}
$$

We may now restate the basic estimation problem as follows: given the observation model of (25), estimate the realization ϕ_k from the observation record $\{z_\ell,\ \ell=1,2,\ldots,k+k_0\}$. This problem is imbedded in a more general MAP sequence estimation problem in Section VIII.

Whenever the discrete-time equations of (25) model an underlying

continuous-time problem, then the parametric links between continuous- and discrete-time are simply

$$\sigma_n^2 = N_0/T \qquad \sigma_W^2 = \sigma_0^2 T \tag{28}$$

These same connections have been used by other authors, based on different arguments. See for example [10]. We have been motivated in our development by the modelling assumptions of Hatsell and Nolte [22].

When there is no underlying continuous-time problem the discrete-time model of (25) becomes a legitimate model in its own right for discrete-time phase tracking. In Section XIV we actually consider some parametric choices for which σ_W^2 is quite large. In these cases the ZOH approximation is not a good one and there is no well-posed underlying continuous-time problem. The phase tracking results should simply be interpreted as discrete-time results for a problem in which the discrete-time phase is rapidly fluctuating.

VIII. The MAP Sequence Estimation Problem

The joint density function of interest is given in (27). Take the ℓn and consider the following MAP sequence estimation problem:

$$\max_{\{\phi_k\}_1^K} \Gamma_K \tag{29}$$

$$\Gamma_K = \frac{1}{\sigma_n^2} \mathrm{Re} \sum_{k=1}^{K} z_k e^{-j\phi_k} + \sum_{k=1}^{K} \ell n\, p(\phi_k/\phi_{k-1})$$

The objective function Γ_K may be written in terms of the envelope and phase variables c_k and ψ_k as follows:

$$\Gamma_K = \frac{1}{\sigma_n^2} \sum_{k=1}^{K} c_k \cos(\psi_k - \phi_k) + \sum_{k=1}^{K} \ell n\, p(\phi_k/\phi_{k-1}) \tag{30}$$

It is clear from the latter form that the MAP phase sequence will be one which stays reasonably close to the noisy phase variables ψ_k (to make cos(·) large) while also maintaining a trajectory that is *a priori* reasonably likely. Thus the MAP sequence strikes a balance between what the noisy data ψ_k *says* the phase is doing and what the transition probabilities $p(\phi_k/\phi_{k-1})$ say the phase *can* do. When the envelope c_k is large there is more of a tendency to believe the measured ψ_k. This curious effect is explained in Section XIII where it is shown that the phase statistic Ψ_k is a modulo-2π unbiased estimate of ϕ_k with a variance that decreases approximately inversely with increasing c_k.

IX. Characteristics of the MAP Sequence

Given the envelope and phase variables $\{c_k\}_1^K$ and $\{\psi_k\}_1^K$, the MAP phase sequence $\{\hat{\phi}_k\}_1^K$ may be obtained by taking derivatives of Γ_K and setting them to zero:

$$\frac{\partial}{\partial \phi_k} \ln p(\hat{\phi}_k/\hat{\phi}_{k-1}) + \frac{\partial}{\partial \phi_k} \ln p(\hat{\phi}_{k+1}/\hat{\phi}_k) + \frac{1}{\sigma_n^2} c_k \sin(\psi_k - \hat{\phi}_k) = 0, \quad k=1,2,\ldots,K \tag{31}$$

The boundary conditions are

$$(1) \quad \frac{\partial}{\partial \phi_1} \ln p(\hat{\phi}_1/\hat{\phi}_0) = 0$$

$$(2) \quad \frac{\partial}{\partial \phi_K} \ln p(\hat{\phi}_{K+1}/\hat{\phi}_K) = 0 \tag{32}$$

Condition (1) simply reflects the fact that $p(\phi_1/\phi_0)$ is uniform on $[-\pi,\pi)$. Condition (2) is a mathematical convenience that allows us to put all the equations of (31) in the same form. Of course $\hat{\phi}_0$ and $\hat{\phi}_{K+1}$ are not computed from the data $\{c_k\}_1^K$ and $\{\psi_k\}_1^K$.

Equations (29) are nonlinear equations with two-point boundary conditions. They are analogous to the continuous-time MAP equations obtained for phase tracking on an interval. While we cannot solve the equations of (31) explicitly we can make some very interesting observations regarding the properties of the MAP phase sequence.

It is easily verified from the conditional density of (8) that

$$\frac{\partial}{\partial \phi_k} \ln p(\phi_{k+1}/\phi_k) = - \frac{\partial}{\partial \phi_{k+1}} \ln p(\phi_{k+1}/\phi_k) \tag{33}$$

Therefore when the K equations of (31) are summed and the boundary conditions applied, all terms involving $\ln p(\hat{\phi}_{k+1}/\hat{\phi}_k)$ cancel. We are

left with the result

$$\sum_{k=1}^{K} c_k \sin(\psi_k - \hat{\phi}_k) = 0 \tag{34}$$

Define the "phase-corrected vector"

$$\hat{\Lambda}_K = \sum_{k=1}^{K} c_k e^{j(\psi_k - \hat{\phi}_k)}$$

and write condition (34) as

$$\text{Im } \hat{\Lambda}_K = 0 \tag{36}$$

This allows us to make the following observation: while maximizing the objective function Γ_K, the MAP sequence $\{\hat{\phi}_k\}_1^K$ yields a maximum value for Γ_K of

$$\hat{\Gamma}_K = \frac{1}{\sigma_n^2} \text{Re } \hat{\Lambda}_K + \sum_{k=1}^{K} \ell n\, p(\hat{\phi}_{k+1}/\hat{\phi}_k) \tag{37}$$

with the property that $\text{Im } \hat{\Lambda}_K = 0$. This property is illustrated in Figure 3. We note that there are many other sequences that satisfy the conditions $\text{Im } \hat{\Lambda}_K = 0$ (e.g. the sequence of maximum likelihood estimates $\hat{\phi}_k = \psi_k$). But these sequences do not also maximize Γ_K.

X. The MAP Sequence for Fixed Phase Acquisition

Suppose the underlying phase sequence $\{\Phi_k\}_1^K$ is known to be a constant sequence with the value of the constant uniformly-distributed on $[-\pi,\pi]$. In this case the MAP sequence estimate is identical with the maximum likelihood (ML) estimate of an unknown phase parameter ϕ in a complex normal model. For this reason, and for the insight it gives into phase estimation, we include in the following paragraphs a short discussion of constant phase and envelope detection in complex normal models. The inclusion of unknown envelope (call it c) generalizes the discussion while not influencing the nature of the phase estimate. This follows from the fact that the phase estimate is uncoupled from the envelope estimate. The converse is not true.

Consider the joint density function for the data $\{Z_k\}_1^K$, parameterized by the envelope c and the phase ϕ:

$$g(\{z_k\}_1^K) = \frac{1}{(2\pi\sigma_n^2)^K} \exp\{-\frac{1}{2\sigma_n^2} \sum_{k=1}^K |z_k - ce^{j\phi}|^2\} \tag{38}$$

This may be written

$$g(\{z_k\}_1^K) = d(\phi,c)h(\{z_k\}_1^K) \exp\{\frac{1}{2\sigma_n^2} \text{Re } ce^{-j\phi} \sum_{k=1}^K z_k\} \tag{39}$$

where

$$\begin{aligned} d(\phi,c) &= \frac{1}{(2\pi\sigma_n^2)^K} \exp\{-\frac{1}{2\sigma_n^2} Kc^2\} \\ h(\{z_k\}_1^K) &= \exp\{-\frac{1}{2\sigma_n^2} \sum_{k=1}^K |z_k|^2\} \end{aligned} \tag{40}$$

It follows from the factorization theorem [24, p. 115] that the complex statistic $K^{-1} \sum_{k=1}^K Z_k$ is sufficient for the parameter pair (c,ϕ). The

ML estimate for the composite parameter $a \triangleq ce^{j\phi}$ is

$$\hat{a} = K^{-1} \sum_{k=1}^{K} z_k \tag{41}$$

The ML estimator is consistent, unbiased, efficient, and minimum variance unbiased. The ML equation for $\hat{c}$ and $\hat{\phi}$ are

$$\hat{c} - K^{-1} \sum_{k=1}^{K} \text{Re}\, z_k e^{j\hat{\phi}} = 0 \tag{42}$$

$$\sum_{k=1}^{K} \text{Re}\, j\, z_k e^{-j\hat{\phi}} = 0 \tag{43}$$

The corresponding ML estimates are

$$\hat{c} = K^{-1} \left| \sum_{k=1}^{K} z_k \right| \tag{44}$$

$$\hat{\phi} = \arg \sum_{k=1}^{K} z_k \tag{45}$$

These estimates are, of course, simply $\hat{c} = |\hat{a}|$ and $\hat{\phi} = \arg \hat{a}$. However (42) and (43) have been presented because they enable us to quickly determine whether or not $\hat{c}$ and $\hat{\phi}$ are efficient. It follows from the linearity of (42) that $\hat{c}$ is efficient (see [6], p. 73). In fact $\hat{c}$ is consistent, unbiased, efficient, and minimum variance unbiased. From the nonlinearity of (43) in the estimate $\hat{\phi}$ we know that the ML phase estimator is not efficient and that no efficient estimator of phase exists. The estimator is consistent. As the discussion to follow shows, the ML estimator of phase is biased. However, it is modulo-2π unbiased, which is the property we want. The phase estimate $\hat{\phi}$, also obtained in [10] in a different way, is illustrated in Fig. 4.

Let $\hat{C}$ and $\hat{\Phi}$ be the estimators corresponding to the estimates $\hat{c}$

and $\hat{\phi}$. We may write

$$K^{-1} \sum_{k=1}^{K} Z_k = \hat{C}e^{j\hat{\phi}} \tag{46}$$

The sufficient statistic $K^{-1} \sum_{k=1}^{K} Z_k$ is $N(ce^{j\phi}, \sigma_n^2/K)$. The Jacobian of the transformation between $(\hat{C},\hat{\phi})$ and $K^{-1} \sum_{k=1}^{K} Z_k$ is $\hat{C}$. Therefore the joint density of $\hat{C}$ and $\hat{\phi}$ is

$$\begin{aligned} g(\hat{c},\hat{\phi}) &= \frac{\hat{c}K}{2\pi\sigma_n^2} \exp\{-\frac{K}{2\sigma_n^2} |\hat{c}e^{j\hat{\phi}} - ce^{j\phi}|^2\} \\ &= \frac{\hat{c}K}{2\pi\sigma_n^2} \exp\{-\frac{K}{2\sigma_n^2} [\hat{c}^2 - 2c\hat{c}\cos(\hat{\phi}-\phi) + c^2]\} \end{aligned} \tag{47}$$

This result is equivalent to (9.46) in [23, p. 413] with appropriate change of notation. In (47) it is assumed $-\pi \le \hat{\phi} \le \pi$. On this interval $g(\hat{c},\hat{\phi})$ is not symmetrical about ϕ and therefore the estimator $\hat{\phi}$ is biased. However we may periodically extend $g(\hat{c},\hat{\phi})$ outside $[-\pi,\pi]$ in order to define the following density on $\phi - \pi \le \hat{\phi} \le \phi + \pi$:

$$g_\phi(\hat{c},\hat{\phi}) = \begin{cases} g(\hat{c},\hat{\phi}) & , \ \phi - \pi \le \hat{\phi} \le \phi + \pi \\ 0 & , \ \text{otherwise} \end{cases} \tag{48}$$

On the RHS of (48) $g(\hat{c},\hat{\phi})$ stands for a periodically extended version of (47). Now $g_\phi(\hat{c},\hat{\phi})$ is symmetrical about ϕ and it is the density of $\hat{\phi}$ measured modulo-2π with respect to ϕ. Thus

$$\int_0^\infty d\hat{c} \int_{\phi-\pi}^{\phi+\pi} (\hat{\phi}-\phi) g_\phi(\hat{c},\hat{\phi}) d\hat{\phi} = 0 \tag{49}$$

which is the modulo-2π unbiasedness property that we want. In (49) it is understood that $\hat{\phi}$ is measured modulo-2π with respect to ϕ.

XI. The Viterbi Algorithm

The MAP sequence estimation problem is stated in (29). Note that Γ_k satisfies the recursion

$$\Gamma_k = \Gamma_{k-1} + \frac{1}{\sigma_n^2} c_k \cos(\psi_k - \hat{\phi}_k) + \ell n\, p(\phi_k/\phi_{k-1})$$
$$\Gamma_1 = \frac{1}{\sigma_n^2} c_1 \cos(\psi_1 - \phi_1) + \ell n\, p(\phi_1/\phi_0) \tag{50}$$

The so-called path metric is

$$\frac{1}{\sigma_n^2} c_k \cos(\psi_k - \hat{\phi}_k) + \ell n\, p(\phi_k/\phi_{k-1}) \tag{51}$$

The maximization problem for obtaining the MAP phase sequence may now be written

$$\max_{\{\phi_k\}_{K-1}^{K}} \left[\max_{\{\phi_k\}_1^{K-2}} \Gamma_{K-1} + \ell n\, p(\phi_K/\phi_{K-1}) + \frac{1}{\sigma_n^2} c_K \cos(\psi_K - \phi_K) \right] \tag{52}$$

This form leads to the following observation: the maximizing trajectory (call it $\{\hat{\phi}_k\}_1^K$), passing through $\hat{\phi}_{K-1}$ on its way to $\hat{\phi}_K$, must arrive at $\hat{\phi}_{K-1}$ along a route $\{\hat{\phi}_k\}_1^{K-2}$ that maximizes Γ_{K-1}. If it did not we could retain $\hat{\phi}_{K-1}$ and $\hat{\phi}_K$ and replace $\{\hat{\phi}_k\}_1^{K-2}$ with a different sequence to get a larger value for Γ_K. It is this observation which forms the basis of forward dynamic problem. The Viterbi algorithm, a forward dynamic programming algorithm applied to MAP sequence estimation on finite-state convolutional sequences, may be applied.

The trellis of Fig. 5 illustrates how the maximization of (52) proceeds. Tabulated values of $p(\phi_k/\phi_{k-1})$ are stored in a square array (or vector which is cyclically read) whose dimensions depend upon how finely the interval $[-\pi,\pi)$ is discretized[4]. Call $\underline{\underline{\Xi}} \times \underline{\underline{\Xi}}$, with $\underline{\underline{\Xi}} = \{\xi_\ell\}_1^M$, the finite-dimensional grid for which $p(\bar{\phi}_k/\bar{\phi}_{k-1})$ is defined. That is, ϕ_k

[4] See the discussion in Section IV.

is assumed to take on only the values $\phi_k = \xi_\ell$, $\ell=1,2,\ldots,M$, for each k. Call $\Gamma_k(\xi_\ell,\xi_m)$ the value of the metric Γ_k corresponding to a phase trajectory $\{\phi_j\}_1^k$ which terminates at phase-state ξ_ℓ at stage k, after passing through stage ξ_m at stage k-1.

The algorithm begins with a computation of $\Gamma_1(\xi_\ell,\xi_\ell)$, $\ell=1,2,\ldots,M$ based on measured values of c_1 and ψ_1. See (50). If all phase values are equally likely *a priori*, then $\ell n\ p(\phi_1/\phi_0)$ is constant on all values ξ_ℓ. Otherwise there is some *a priori* weighting in favor of some of the ξ_ℓ. A new measurement pair (c_2,ψ_2) is obtained at k=2 and $\Gamma_2(\xi_1,\xi_m)$ is computed for m=1,2,...,M using a table look-up (e.g. in ROM) for the $p(\phi_2=\xi_1/\phi_1=\xi_m)$. The maximum value of $\Gamma_2(\xi_1,\xi_m)$ is determined (the maximization is over all originating states ξ_m) and the corresponding sequence $(\xi_1,\hat{\xi}_1)$ is saved as a *survivor* sequence terminating at ξ_1 at stage 2; $\hat{\xi}_1$ denotes the originating state. The survivor sequence is labelled with its corresponding *length* $\Gamma_2(\xi_1,\hat{\xi}_1)$. This calculation is repeated for each possible value of phase until all pairs $(\xi_\ell,\hat{\xi}_\ell)$, and corresponding lengths $\Gamma_2(\xi_\ell,\hat{\xi}_\ell)$, $\ell=1,2,\ldots,M$, have been computed and stored in soft memory (e.g. RAM). There is a unique survivor sequence corresponding to each state ξ_ℓ, $\ell=1,2,\ldots,M$. *Caution:* In the pair $(\xi_\ell,\hat{\xi}_\ell)$ the originating state $\hat{\xi}_\ell$ depends on ξ_ℓ; i.e., $\hat{\xi}_\ell = \hat{\xi}_\ell(\xi_\ell)$. The measurements c_2 and ψ_2 may now be discarded along with all extinct sequences. Now a new measurement pair (c_3,ψ_3) is obtained and $\Gamma_3(\xi_1,\xi_m)$ is computed for m = 1,2,...,M using the recursion for Γ_k and a table look-up for $p(\phi_3=\xi_1/\phi_2=\xi_m)$. The maximizing value of $\Gamma_3(\xi_1,\xi_\ell)$, call it $\Gamma_3(\xi_1,\hat{\xi}_1)$ is computed and the corresponding triple $(\xi_1,\hat{\xi}_1,\cdot)$ is stored as a survivor sequence originating in $(\cdot)$ at stage 1, passing through $\hat{\xi}_1$ at stage 2, and terminating in ξ_1 at stage 3. This procedure is

repeated until M survivor sequences of the form $(\xi_\ell, \hat{\xi}_\ell, \cdot)$ are determined and stored with their respective survivor metrics $\Gamma_3(\xi_\ell, \hat{\xi}_\ell, \cdot)$. The measurements (c_3, ψ_3) and all extinct sequences may be discarded.

Call $(\hat{\phi}_1(k), \hat{\phi}_2(k), \ldots, \hat{\phi}_k(k))$ the MAP sequence based on k measurements up to stage k. This sequence has the maximum value of Γ_k. The parenthetical notation (k) denotes dependence on measurement interval. In general the MAP sequence estimate, $(\hat{\phi}_1(k+1), \ldots, \hat{\phi}_{k+1}(k+1)$, based on measurements up to stage k+1, may differ from the previous sequence estimate at every stage from 1 to k. However, as a practical matter, one can choose a sufficiently large depth parameter k_0 so that the sequence of fixed-lag estimates

$$\hat{\phi}_{k-k_0}(k) \quad , \quad k = k_0+1,\ k_0+2, \ldots \tag{53}$$

gives an approximate MAP sequence estimate. Here $\hat{\phi}_{k-k_0}(k)$ is simply the phase value, k_0 stages back, in the MAP sequence estimate based on k measurements. In this way one obtains a phase track with delay k_0.

Following Forney []5] we may summarize the storage and computational requirements for the phase tracking algorithm as follows:

Storage

k	(time index)
$(\xi_\ell, \xi_\ell, \cdot, \ldots), \ell=1,2,\ldots,M$	(survivor phase sequence terminating in ξ_ℓ at stage k)
$\Gamma_k(\xi_\ell, \hat{\xi}_\ell, \ldots), \ell=1,2,\ldots,M$	(survivor metric)
$p(\xi_\ell/\xi_m), \ell=1,\ldots,M$ $m=1,\ldots M$	(transition probability matrix)

Initialization

$k = 1$

$\hat{\xi}_\ell = \xi_\ell, \ \ell=1,\ldots,M$

$$\Gamma_1(\xi_\ell, \hat{\xi}_\ell) = \ln p(\phi_1=\xi_\ell/\phi_0) + \frac{1}{2\sigma_n^2} 2c_1 \cos(\psi_1-\xi_\ell), \ \ell=1,2,\ldots,M$$

Recursion

$$\Gamma_{k+1}(\xi_\ell,\xi_m) = \Gamma_k(\xi_m,\hat{\xi}_m) + \ln p(\phi_{k+1}=\xi_\ell/\phi_k=\xi_m) + \frac{1}{2\sigma_n^2} 2c_{k+1}\cos(\psi_{k+1}-\xi_\ell),\ \ell=1,2,\ldots,M$$

$$\min_{\{\xi_m\}} \Gamma_{k+1}(\xi_\ell,\xi_m)\ ,\quad \ell=1,2,\ldots,M$$

Measurement/Computation

c_k	envelope
ψ_k	phase
$c_k\cos(\xi_\ell-\psi_k) + \ln p(\phi_k=\xi_\ell/\phi_{k-1}=\xi_m)$	path metric

In Fig. 5 typical trajectories for this algorithm are illustrated. The heavy lines denote survivors and the light lines denote path metric calculations that are made and then discarded in favor of survivors. At stage 3 all calculations $\Gamma_3(\xi_2,\xi_m)$ are illustrated with light lines; the heavy line from ξ_3 to ξ_2 illustrates that this path gives maximum $\Gamma_2(\xi_2,\xi_m)$ and is therefore labelled a survivor. Of course $\hat{\xi}_2 = \xi_3$. The x's on the trellis illustrate sequences that have survived for a while before being exterminated by the weight of evidence. The very heavy line at each measurement stage k denotes the current MAP sequence. The circled numbers denote the current MAP sequence. The sequence of end points labelled with the circled numbers is a sequence of *phase estimates*. Note this *sequence of phase estimates* differs from the *MAP phase sequence estimate*. The latter, being a smoothing solution, is in fact generally smoother than the former.

XII. Illustrative Simulations

In the simulations described here the phase space $[-\pi,\pi)$ has been discretized to M points $\xi_\ell = \ell 2\pi/M - (M-1)\pi/M$, $\ell=1,2,\ldots,M$. In Figures 6 and 7, M=11. In Figure 8, M=17. The conditional probabilities between states have been approximated with the normalized version of (8) discussed in Section IV. These values have been stored in an MxM matrix (really an M-vector which is cyclically permuted to generate the rows of the Toeplitz transition matrix) and used to calculate path metrics according to (51).

A random walk phase sequence was generated from (26) and used to construct a sequence of measurements according to (25). The measurements were then used in the dynamic programming algorithm of Section XI to generate the results of Figures 6-8.

Fig. 6 is a relatively high signal-noise ratio example where $\sigma_n^2 = 0.1$ (S/N = 10dB). The phase variance parameter is $\sigma_w^2 = (\pi/10\sqrt{2})^2$, corresponding to a phase trajectory whose "1-σ transitions" are on the order of $\pi/14$. In Fig. 6 the solid curve with piecewise constant slopes is the actual phase sequence $\{\phi_k\}$. The dotted curve with piecewise constant slopes is the measurement sequence $\{\psi_k\}$ with $\psi_k = \arg z_k \in [-\pi,\pi)$. The heavy lines labelled with numbers from 1 to 37 are MAP phase sequences[5] generated with the Viterbi algorithm of Section XI. The MAP sequence after k measurements is labelled with the corresponding k value at the end of the sequence. Note in the Figure that the maximum number of phase corrections to a path is 4, occurring at measurement 9. There is a correction of 3 phase values at measurement 27, in a region of very noisy measurements. Thus for this

[5] Of course these are not really MAP sequences because of the approximations inherent in our discretization of the phase space. But it is cumberson and confusing to continually refer to the sequences as *approximate* MAP sequences.

simulation one could have decoded the MAP sequence corresponding to 37 measurements by decoding with a fixed delay (or depth constant) of $k_0 = 4$. See the discussion surrounding (53).

Fig. 7 shows a simulation for $\sigma_n^2 = 0.5$, corresponding to a signal-noise ratio of -3dB. The phase sequence $\{\phi_k\}$ is somewhat more wildly fluctuating than in the previous case: $\sigma_w^2 = (\pi/10)^2$. The measurement sequence is really not underbiased as it appears to be. Noisy measurements on a phase sequence that hugs the upper boundary of $[-\pi,\pi)$ are bound to *appear* underbiased because of the way the measurement $\psi_k = \arg z_k \in [-\pi,\pi)$ is computed. Several measurements in the vicinity of k = 28-39 are reflected upward by 2π to further clarify this point.

The simulation of Fig. 7 illustrates how the Viterbi tracker acquires phase at low signal-noise ratios. Note that early on in the run the algorithm jumps wildly between the phase points 1 (at k=1), 11 (at k=2), 9 (at k=3,4),...6 (at k=8), and so on. Furthermore, the MAP trajectories in this phase acquisition region are constant phase trajectories that have high *a priori* probability; i.e., the transition from $\phi_k = \xi_\ell$ to $\phi_{k+1} = \xi_\ell$ is more probable than any other. It should also be noted that the MAP sequences at k=21-24 are actually quite good - the modulo-2π errors between the sequence values and the actual phase are small. Finally, note that for k=25 and 26 the algorithm has been diverted from the actual phase by a sequence of unusually noisy measurements. By measurement k=27 this situation has been recognized and a new trajectory that is constant through the period of noisy measurements has been constructed. This behavior is characteristic of the algorithm and is, in fact, one of the very nice features of the algorithm.

Fig. 8 illustrates how the algorithm operates on wild phase sequences that make excursions outside the interval $[-\pi,\pi)$. For this example the phase variance parameter is large : $\sigma_w^2 = (\pi/5)^2$. In the course of 45 sampling instants the actual phase sequence $\{\phi_k\}$ wanders over a range of 3π radians. For clarity of presentation phase values lying outside $[-\pi,\pi)$ have been reflected inside so that performance of the modulo-2π phase tracker may be correctly gauged. If loss of phase lock is defined to be a phase error of π radians, then none occur. If it is defined to be $\pi/2$, then 2 occur in the vicinity of k=25, in a region of very wild phase fluctuations.

XIII. The Phase Locked Loop and Kalman Filter Performance Bounds

The phase locked loop (PLL) for the discrete-time problem posed in (25) is [10]

$$\hat{\phi}_k = \hat{\phi}_{k-1} + (\sigma_w^2/\sigma_n^2)^{\frac{1}{2}} \operatorname{Im} z_k e^{-j\hat{\phi}_{k-1}}$$
$$= \hat{\phi}_{k-1} + (\sigma_w^2/\sigma_n^2)^{\frac{1}{2}} c_k \sin(\psi_k - \hat{\phi}_{k-1}) \tag{54}$$

Here $\hat{\phi}_k$ denotes an estimate of the phase ϕ_k based on measurements $\{z_\ell\}_1^k$. The result of (54), illustrated in Figure 9, may be interpreted as an extended Kalman filter with measurement dependent gain $K_k = (\sigma_w^2/\sigma_n^2)^{\frac{1}{2}} c_k$. As with the MAP sequence estimate of Sections IX-XI, data is given more weight for large values of the envelope c_k than for small values. A probabilistic justification goes as follows. The conditional density of the phase statistic Ψ_k, given $C_k = c_k$, and ϕ_k is

$$f(\psi_k/c_k) = \frac{1}{2\pi} I_0^{-1}(\beta^{-1}) \exp\{\beta^{-1}\cos(\psi_k - \phi_k)\}, \quad \psi_k - \phi_k \in [-\pi, \pi)$$
$$\beta = \sigma_n^2/c_k \tag{55}$$

This density is symmetric about ϕ_k so that

$$E[\Psi_k/c_k] = \phi_k \tag{56}$$

where the expectation is a "modulo-2π expectation". See the discussion of Section X. The modulo-2π conditional variance of Ψ_k, denoted $\operatorname{var}[\Psi_k/c_k]$, may be numerically evaluated. The result is plotted in Figure 10. The important asymptotic results are

$$\text{var}[\Psi_k/c_k] = \begin{cases} \pi^2/3 & , \quad \beta \to \infty \\ \beta & , \quad \beta \to 0 \end{cases} \tag{57}$$

Thus the conditional variance of the modulo-2π unbiased phase statistic Ψ_k is small for large values of c_k/σ_n^2. This justifies heavy weighting of new measurements.

The performance of the PLL may be analyzed by appealing to a known result obtained by Viterbi for a related continuous-time problem. Under the conditon that $\sigma_w^2/\sigma_n^2 \leq 0.01$, the result is that the steady-state error performance for the PLL is well-approximated by [10]

$$\sigma^2 = \int_{-\pi}^{\pi} x^2 \, \frac{1}{2\pi} \, I_0^{-1}(r^{-1}) \exp(r^{-1}\cos x) \, dx$$
$$r = (\sigma_w^2\sigma_n^2)^{\frac{1}{2}} \tag{58}$$

The asymptotics are

$$\sigma^2 = \begin{cases} \pi^2/3 & , \quad r \to \infty \\ r & , \quad r \to 0 \end{cases} \tag{59}$$

Thus the performance of the PLL follows the same curve as the conditional variance of Ψ_k, with β replaced by r. See Figure 10. At high input signal-noise ratio ($\sigma_n^2 << 1$ and $\beta << 1$) the variance of Ψ_k is approximately β; the variance of the PLL estimate is $(\sigma_w^2\sigma_n^2)^{\frac{1}{2}}$. Thus the *gain* of the PLL is the ratio of these variances,

$$G = c_k(\sigma_w^2/\sigma_n^2)^{\frac{1}{2}} \tag{60}$$

which is, of course, the weighting applied to the error term $\sin(\psi_k - \hat{\phi}_k)$ in (54).

To pursue this analysis further we note that when $\sigma_n^2 << 1$, c_k will

be near unity with high probability and $\sin(\psi_k-\hat{\phi}_k)$ will be well-approximated by $(\psi_k-\hat{\phi}_k)$. In this so-called linear region of operation the PLL performs as if it were forming the estimates

$$\hat{\phi}_k = \hat{\phi}_{k-1} + (\sigma_w^2/\sigma_n^2)\ (\psi_k-\hat{\phi}_k) \tag{61}$$

As we now show this is approximately the Kalman filter for a linear problem when $\sigma_w^2/\sigma_n^2 \leq 0.01$.

Consider the linear problem

$$\begin{aligned} \Psi_k &= \Phi_k + N_k \ ; \ N_k \ : \ N(0,\sigma_n^2) \\ \Phi_k &= \Phi_{k-1} + W_k \ ; \ W_k \ : \ N(0,\sigma_w^2) \end{aligned} \tag{62}$$

The steady-state Kalman filter for this problem is

$$\hat{\phi}_k = \hat{\phi}_{k-1} + (\sigma^2/\sigma_n^2)\ (\psi_k-\hat{\phi}_{k-1}) \tag{63}$$

where σ^2 is the steady-state filtering error and σ^2/σ_n^2 is the Kalman gain. This error is easily shown to be

$$\sigma^2 = \sigma_w^2[-\tfrac{1}{2} + \tfrac{1}{2}(1+4\sigma_n^2/\sigma_w^2)^{1/2}] \tag{64}$$

The filtering error is plotted versus $(\sigma_w^2\sigma_n^2)^{1/2}$ for several values of σ_w^2 in Figure 11. Note that when $\sigma_w^2/\sigma_n^2 \leq 0.01$, σ^2 is well-approximated by

$$\sigma^2 = (\sigma_w^2\sigma_n^2)^{1/2} \qquad (=r) \tag{65}$$

and the Kalman gain is $(\sigma_w^2/\sigma_n^2)^{1/2}$ just as in (61). This means that under the assumptions $\sigma_w^2/\sigma_n^2 \leq 0.01$ *and* $\sigma_n^2 << 1$, the PLL is essentially a Kalman filter whose estimated phase variance is $\sigma^2 = (\sigma_w^2\sigma_n^2)^{1/2}$. Therefore the curves outlining the hatched region of Figure 11 nicely bound achievable performance for a PLL when $\sigma_w^2/\sigma_n^2 < 0.01$, and the most

natural way of presenting performance curves is to plot them versus $(\sigma_w^2\sigma_n^2)^{\frac{1}{2}}$. The assumption $\sigma_w^2/\sigma_n^2 \leq 0.01$ is made in all current literature on discrete-time phase tracking, so all performance results lie in the hatched region. This region corresponds to low signal-noise ratios and slowly fluctuating phase sequences.

At all values of σ_w^2/σ_n^2 and σ_n^2 the Kalman filter performance results of (64) and Figure 11 lower bound the achievable performance for a PLL or any other filtering structure, nonlinear or not. In Section XIV we present performance results for problems in which these curves are the appropriate bounding curves. It must be remembered when interpreting results that a given value of $r = (\sigma_w^2\sigma_n^2)^{\frac{1}{2}}$ corresponds to a smaller value of σ_n^2 (and higher signal-noise ratio) when $\sigma_w^2/\sigma_n^2 > 0.01$ than when $\sigma_w^2/\sigma_n^2 \leq 0.01$.

XIV. Performance Results and Comparisons with Other Nonlinear Trackers

The phase space $[-\pi,\pi)$ has been discretized to M=11 equally-spaced points and the Viterbi algorithm for phase tracking implemented as outlined in Section XI. The crucial conditional probabilities $p(\phi_k=\xi_m/\phi_{k-1}=\xi_\ell)$ have been computed as outlined in Section IV and stored in an M vector for cyclic reading. Random phase trajectories and measurement variables have been generated according to (25) and (26). The results of several Monte-Carlo simulations are presented in TABLE I and Figures 12 and 13. Each Monte-Carlo result has been obtained by running the Viterbi phase tracker (and the PLL) over 40 different trajectories, each trajectory beginning with a uniformly-distributed phase variable at k=1 and continuing for 500 points. Various values of depth parameter k_0 have been used, as indicated in the figures. Refer to [10] for a discussion of corresponding statistical sampling errors.

All simulations have been run on a UNIVAC 1110. The run time for a Monte-Carlo experiment consisting of 20,000 points is 66 sec., a figure that includes computation of Monte-Carlo statistics but excludes a fixed compilation time of 28 sec. for the program. The number of estimates per second produced by the algorithm is approximately 300/sec., making the algorithm 150 times faster than the PMF of [10] and approximately 20 times faster than the Fourier implementation of the PMF reported in [13].

TABLE I shows numerical results for the sample filtering variance in rad^2 for the Viterbi phase tracker. For all entries the depth constant was k_0=10, meaning the filter ran as a fixed lag smoother with a lag of 10 samples. Each Monte-Carlo result for σ^2 was obtained from 20,000 estimates of phase.

In Figure 12 Monte-Carlo simulation results for the Viterbi tracker

are presented for the parametrizations commonly considered in the literature. The results are compared with the PMF [10], the FCF [9], the LQF [11], and the GSF [15]. Also shown are our simulation results for the PLL. These results are presented to legitimize the simulation. For a depth constant of k_0=10 the Viterbi tracker outperforms the PMF by approximately 0.5 dB at r=1.0 (0dB). Furthermore the Viterbi tracker makes up more than 1.0 of the 2.0 dB performance gap between the PLL and an idealized linear tracker. In terms of rms phase error (in radians), the comparison between the PLL and the Viterbi tracker goes as follows. The PLL has an rms phase error of 1.26 rad at r=1.0. The maximum achievable percentage improvement is 21%, corresponding to an ideal filter with rms phase error of 1.0 rad. The rms error for the Viterbi tracker operating at r=1.0 with k_0=10 is 1.12. This represents an improvement of 11% over the PLL. The results for k_0=0 show that (as expected) the Viterbi tracker is not as good as a PLL as a zero-lag filter. In Figure 12 the heavy squares denoted by VT(MAP) (see the symbol key) correspond to the smoothing variance achieved when the MAP sequence for a 500 sample run is used as the phase estimate. The results are averaged over 40 such runs. The tabulated results in Figure 12 summarize the performance characteristics of many different nonlinear phase trackers. In the Figure, performance results for the Viterbi tracker are plotted just to the left of their true positions to avoid cluttering the presentation.

Figure 13 contains Monte-Carlo performance results for parameter cases not usually considered. These results, generally corresponding to high signal-noise ratio and rapidly varying phase cases, may be of interest in data communications applications where phase jitter is a serious problem. The results of Figure 13 show the Kalman filter

performance bounds to be useful as fairly tight lower bounds on observed performance. At $\sigma_n^2 = 0.10$ (10dB signal-noise ratio), and $\sigma_w^2 = 1.0$, in which case the PLL is unstable, the Viterbi tracker performs within 1 dB of an idealized linear tracker. See the black squares at r = -5dB. At $\sigma_n^2 = 1.0$ (0 dB signal-noise ratio), and $\sigma_w^2 = 0.10$, the Viterbi tracker achieves essentially ideal performance for $k_0 = 10$ while outperforming the PLL by slightly more than 2 dB. See the white squares at r = -5dB. Similar performance interpretations hold for $\sigma_n^2 = 1.0$ when $\sigma_w^2 = 0.01$ and $\sigma_w^2 = 1.0$. In the latter case the PLL is outperformed by about 3dB.

We hasten to emphasize in the interest of fairplay that all results presented here for non-zero k_0 are in reality smoothing solutions. Such solutions are expected to outperform filtering solutions. This does not detract from the fixed lag Viterbi tracker as an attractive alternative in those applications where a short delay may be accepted in exchange for 1-3 dB performance gains.

XV. Applications to Data Communication

An appropriate modification of (25) to model data communication over a perfectly equalized channel is

$$Z_k = I_k e^{j\Phi_k} + N_k \tag{66}$$

Here $\{I_k\}$ may be a sequence of binary of M-ary source symbols which may or may not have been trellis or convolutional encoded. In the simplest case $\{I_k\}$ is an uncoded sequence of independent source symbols drawn from an equiprobable symbol alphabet.

To model data transmission over an imperfectly equalized channel with finite-length pulse response we proceed as follows. Let $\bar{X}_k'$ denote the following (L+1) - tuple of phased symbols:

$$\bar{X}_k' = (I_k e^{j\Phi_k}, I_{k-1} e^{j\Phi_{k-1}}, \ldots, I_{k-L} e^{j\Phi_{k-L}}) \tag{67}$$

Denote by $\bar{r}'$ the finite pulse response of the channel:

$$\bar{r}' = (r_0, r_1, \ldots, r_L) \tag{68}$$

In these definitions the superscript $'$ denotes transposition.

The noisy, complex demodulated channel output at time k may be written

$$Z_k = \bar{r}' \bar{X}_k + N_k \tag{69}$$

In the discussion below we present two examples requiring successively higher levels of complexity for simultaneous phase tracking and symbol decoding. The principle of optimality chosen in these examples is *MAP data sequence/phase sequence estimation*. No claim of minimum symbol error probability or minimum block error probability is made.

Example 1: $\{I_k\}$ is a sequence of independent symbols drawn from an M symbol complex alphabet and transmitted over a perfectly equalized channel. This example includes such modulation schemes as M-ary ASK,

PSK, QASK, etc. The number of candidate message sequences after K symboling periods is M^K.

The appropriate log density function for this example is[7]

$$\log f(\{z_k\}_1^K, \{\phi_k\}_1^K, \{I_k\}_1^K)$$

$$= \log f(\{z_k\}_1^K/\{\phi_k\}_1^K, \{I_k\}_1^K) + \log p(\{\phi_k\}_1^K) \tag{70}$$

$$= C + \frac{1}{2\sigma_n^2} \sum_{k=1}^{K} |z_k - I_k e^{j\phi_k}|^2 + \sum_{k=1}^{K} \log p(\phi_k/\phi_{k-1})$$

It follows easily that the path metric is

$$-\frac{1}{2\sigma_n^2} |z_k - I_k e^{j\phi_k}|^2 + \log p(\phi_k/\phi_{k-1}) \tag{71}$$

This may be written (ignoring terms independent of ϕ_k, I_k)

$$\frac{1}{2\sigma_n^2} 2\mathrm{Re}\, z_k I_k^* e^{-j\phi_k} - \frac{1}{2\sigma_n^2} |I_k|^2 + \log p(\phi_k/\phi_{k-1}) \tag{72}$$

An even more explicit form of the path metric is

$$\frac{1}{2\sigma_n^2} 2 c_k |I_k| \cos(\psi_k - \phi_k - \theta_k) - \frac{1}{2\sigma_n^2} |I_k|^2 + \log p(\phi_k/\phi_{k-1}) \tag{73}$$

where (c_k, ψ_k) are the envelope and phase variables defined previously and $|I_k|$ and θ_k are the magnitude and phase (usually visualized in a complex signal constellation) of the complex symbol I_k. From all three of the forms for the path metric it is clear that one is attempting to reconstruct phase-corrected symbols $I_k^* e^{-j\phi_k}$ that correlate well with the

---

[7] This is actually a mixed density-probability mass function. However because the probability mass function for $\{I_k\}_1^K$ assigns uniform mass M^{-K} to each K-tuple $\{I_k\}_1^K$, we ignore this term and call $f(\cdot,\cdot,\cdot)$ a density.

received data while also satisfying a smoothness constraint (as embodied in the $p(\phi_k/\phi_{k-1})$) on the mod-2π phase sequence.

The appropriate trellis for Viterbi decoding of the modulo-2 phase sequence *and* the symbol sequence is the MxM symbol-phase trellis of pairs (I^m, ξ_ℓ), m=1,2,...,M, ℓ=1,2,...,M, corresponding to all allowable pairs of symbol and phase. Recall M denotes the number of phase points in the discretized modulo-2π phase space. If I_k is drawn from a binary alphabet for all k, then the symbol-phase trellis simply consists of 2M symbol-phase pairs over which survivor sequences are formed as outlined in Section VI.

Example 2: $\{I_k\}$ a sequence of independent symbols drawn from an M symbol complex alphabet and transmitted over a channel with finite pulse response $\{r_\ell\}_0^L$. For this example the appropriate log-density for the K measurements $\{z_k\}_1^K$ is (neglecting uninteresting constants)

$$\log f(\{z_k\}_1^K, \{\phi_k\}_1^K, \{I_k\}_1^K) = \tag{74}$$

$$-\frac{1}{2\sigma_n^2} \sum_{k=1}^{K} |z_k - \bar{r}' \bar{X}_k|^2 + \sum_{k=1}^{K} \log p(\phi_k/\phi_{k-1})$$

Recall $\bar{X}_k$ depends on a specific set of source symbols and phases as in (67). If the modulo 2π phase space $[-\pi,\pi)$ is discretized to M values then there are $(MxM)^{L+1}$ distinct vectors $\bar{X}_k$.

The path matric for this problem is simply

$$-\frac{1}{2\sigma^2} |z_k - \bar{r}'\bar{X}_k|^2 + \log p(\phi_k/\phi_{k-1}) \tag{75}$$

The trellis for Viterbi decoding consists of the $(MxM)^{L+1}$ allowable $\bar{X}$-vectors corresponding to $(MxM)^{L+1}$ distinct phase-symbol strings of length L+1. The path metric for each *allowable* transition in this

trellis is computed as in (75) and used to construct survivor sequences. Of course, not all transitions are allowable because specification of $(I_k, I_{k-1}, \ldots, I_{k-L})$ restricts the next allowable sequence to one of M sequences beginning with I_{k+1} and terminating in I_k through I_{k-L+1}. This means one must store $(MxM)^{L+1}$ survivors and compute path metrics for MxM^{L+1} x $M^{L+1}xM$ allowable transitions.

XVI. Conclusions

We have derived a Viterbi algorithm for obtaining approximate MAP phase sequence estimates on $[-\pi,\pi)$. The algorithm is simple and fast by nonlinear filtering standards, and ideally organized for hardware implementation. Performance is superior to that of existing structures for moderate values of filtering delay, making the approach attractive in applications where delay is acceptable.

Acknowledgments

The authors acknowledge the support of J. Lord, R. McGough, and B. Picinbono. O. Macchi is acknowledged for her helpful discussion and for her critique of the manuscript. C. Pariente conducted the Monte-Carlo simulations at the University of Paris-Sud, using software originally developed by CJM.

References

[1] F. Lehan and R. Parks, "Optimum Demodulation," IRE National Convention Record, part 8, pp. 101-103 (1953).

[2] D. C. Youla, "The Use of Maximum Likelihood in Estimating Continuously Modulated Intelligence Which Has Been Corrupted by Noise," IRE Trans. Inform. Theory, IT-3, pp. 90-105 (March 1954).

[3] R. Bellman, Invariant Imbedding, Academic Press, N.Y. (1964).

[4] D. M. Detchmendy and R. Sridhar, "Sequential Estimation of States and Parameters in Noisy Dynamical Systems," ASME J. Basic Eng., pp. 362-368 (June 1966).

[5] A. B. Baggeroer, "Nonlinear MAP Interval Estimation," Research Laboratory of Electronics, MIT, Cambridge, MA, QPR No. 85, pp. 249-253 (April 1967).

[6] H. L. Van Trees, Detection, Estimation, and Modulation Theory, Part II, N.Y.: Wiley (1971), Ch. 7.

[7] H. J. Kushner, "On the Differential Equations Satisfied by Conditional Probability Densities of Markov Processes, with Applications," J. SIAM Control, Ser. A, 2, pp. 106-119 (1964).

[8] D. Snyder, "The State Variable Approach to Continuous Estimation with Applications to Analog Communication Theory," MIT Press, Cambridge, MA (1969).

[9] A. S. Willsky, "Fourier Series and Estimation on the Circle with Applications to Synchronous Communication - Part I: Analysis," IEEE Trans. Inform. Theory, IT-20, pp. 577-583 (September 1974).

[10] R. S. Bucy and A. J. Mallinckrodt, "An Optimal Phase Demodulator," Stochastics, 1, pp. 3-23 (1973).

[11] D. E. Gustafson and J. L. Speyer, "Linear Minimum Variance Filters Applied to Carrier Tracking," IEEE Trans. on Autom. Contr., AC-21, pp. 65-73 (February 1976).

[12] C. N. Kelly and S. C. Gupta, "The Digital Phase-Locked Loop as a Near-Optimum FM Demodulator," IEEE Trans. Commun., COM-20, pp. 406-411 (June 1972).

[13] R. S. Bucy and H. Youssef, "Fourier Realization of the Optimal Phase Demodulator," Symposium on Nonlinear Estimation and Its Applications, San Diego, CA (1973).

[14] H. W. Sorenson and D. L. Alspach, "Recursive Bayesian Estimation Using Gaussian Sums," Automatic, 7, pp. 465-479 (1971).

[15] P.K.S. Tam and J. B. Moore, "A Gaussian Sum Approach to Phase and Frequency Estimation," IEEE Trans. Commun., COM-25, pp. 935-942 (September 1977).

[16] A. J. Viterbi, "Error Bounds for Convolutional Codes and An Asymptotically Optimum Decoding Algorithm," IEEE Trans. Inform. Theory, IT-15, pp. 260-269 (April 1969).

[17] C. R. Cahn, "Phase Tracking and Demodulation with Delay," IEEE Trans. Inform. Theory, IT-20, pp. 50-58 (January 1974).

[18] G. Ungerboeck, "New Applications for the Viterbi Algorithm" Carrier Phase Tracking in Synchronous Data-Transmission Systems," National Telecommunications Conference (1974).

[19] W. Feller, Introduction to Probability Theory and Its Applications, Vol. II, 2nd Edition, N.Y.: Wiley (1966).

[20] S. Karlin and H. Taylor, "A First Course in Stochastic Processes, 2nd Edition, N.Y.: Academic Press (1975).

[21] H. L. Van Trees, Detection, Estimation, and Modulation Theory, Part I, N.Y.: Wiley (1968), Ch. 4.

[22] C. P. Hatsell and L. W. Nolte, "Optimal Detection of a Signal with Time-Varying Carrier Phase," IEEE Trans. on Aerospace and Electr. Syst., AES-10, pp. 788-794 (November 1974).

[23] D. Middleton, An Introduction to Statistical Communication Theory, N.Y.: McGraw-Hill (1960).

[24] T. S. Ferguson, Mathematical Statistics: A Decision Theoretic Approach, N.Y.: Academic Press (1967).

List of Figures and Tables

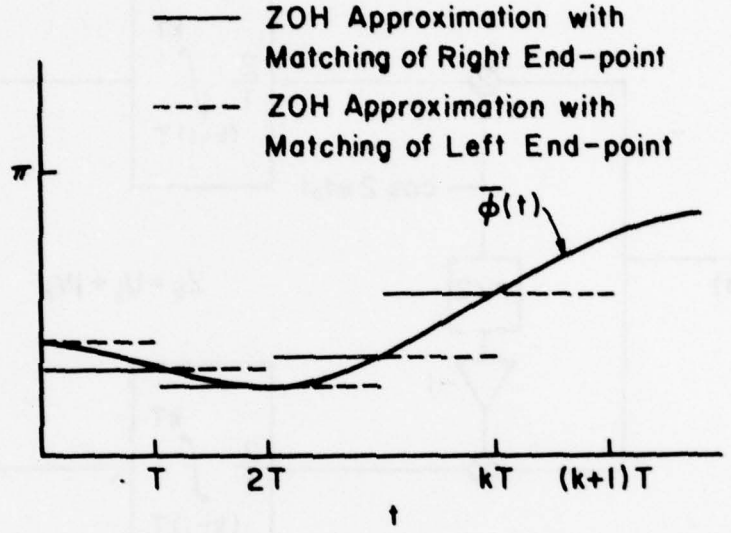

Figure 1. Phase Processes

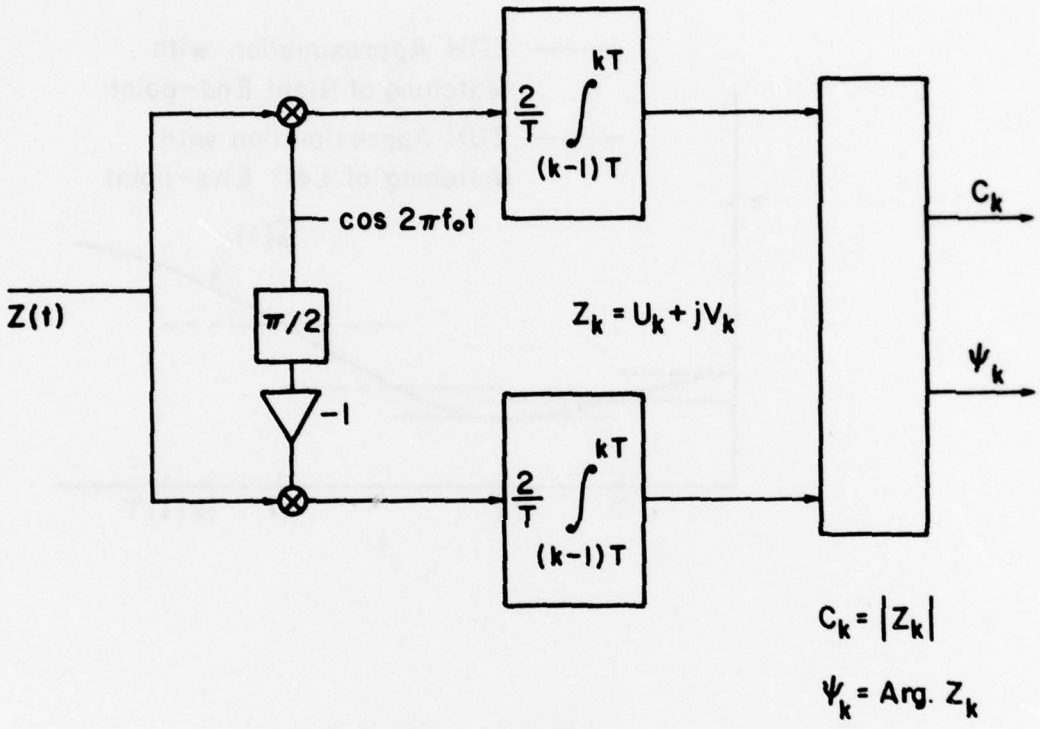

Figure 2. Quadrature Demodulator

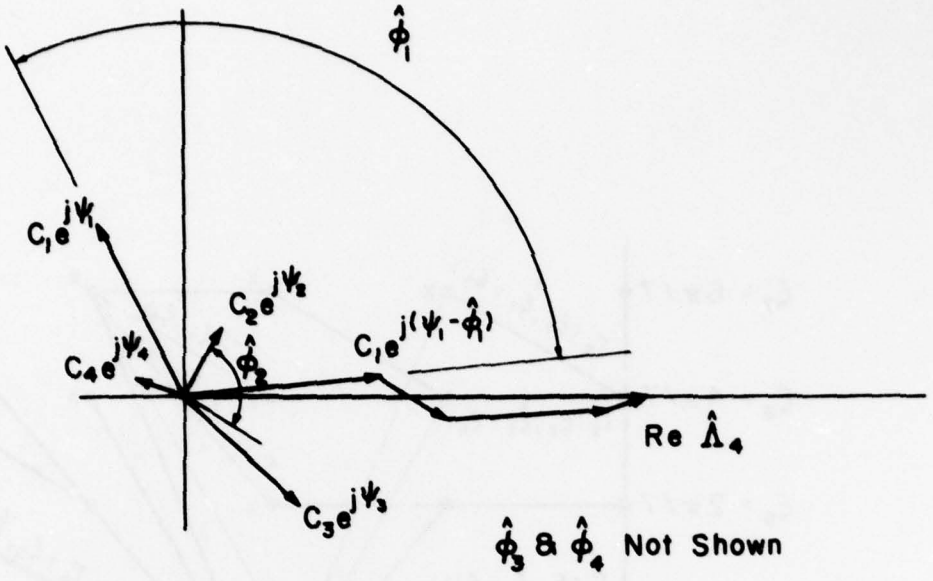

Figure 3. The Nature of the MAP Sequence

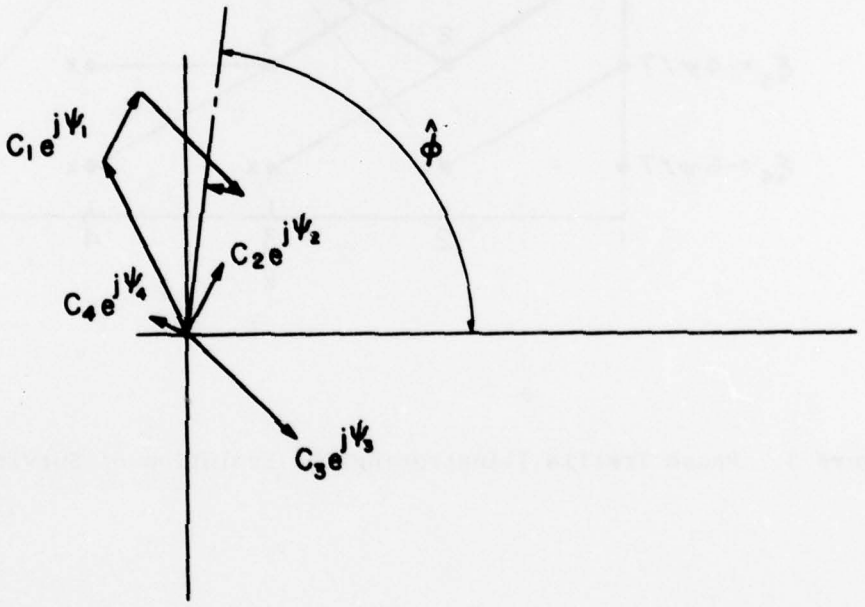

Figure 4. The MAP Estimate for Fixed Phase Acquisition

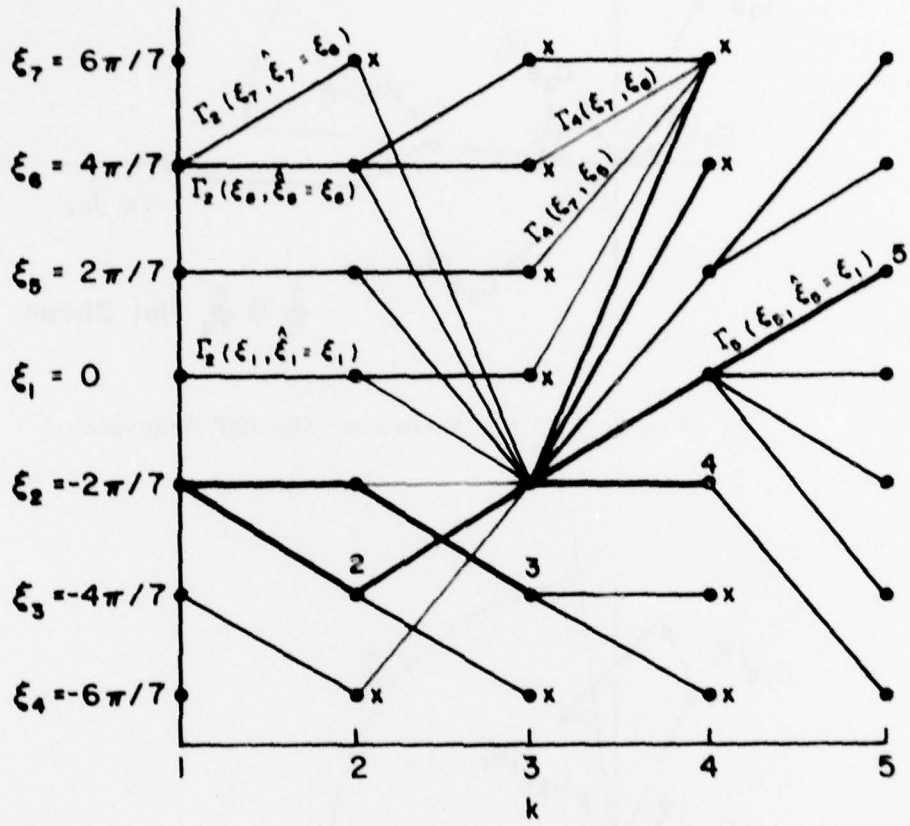

Figure 5. Phase Trellis Illustrating the Evolution of Surviving Phase Tracks

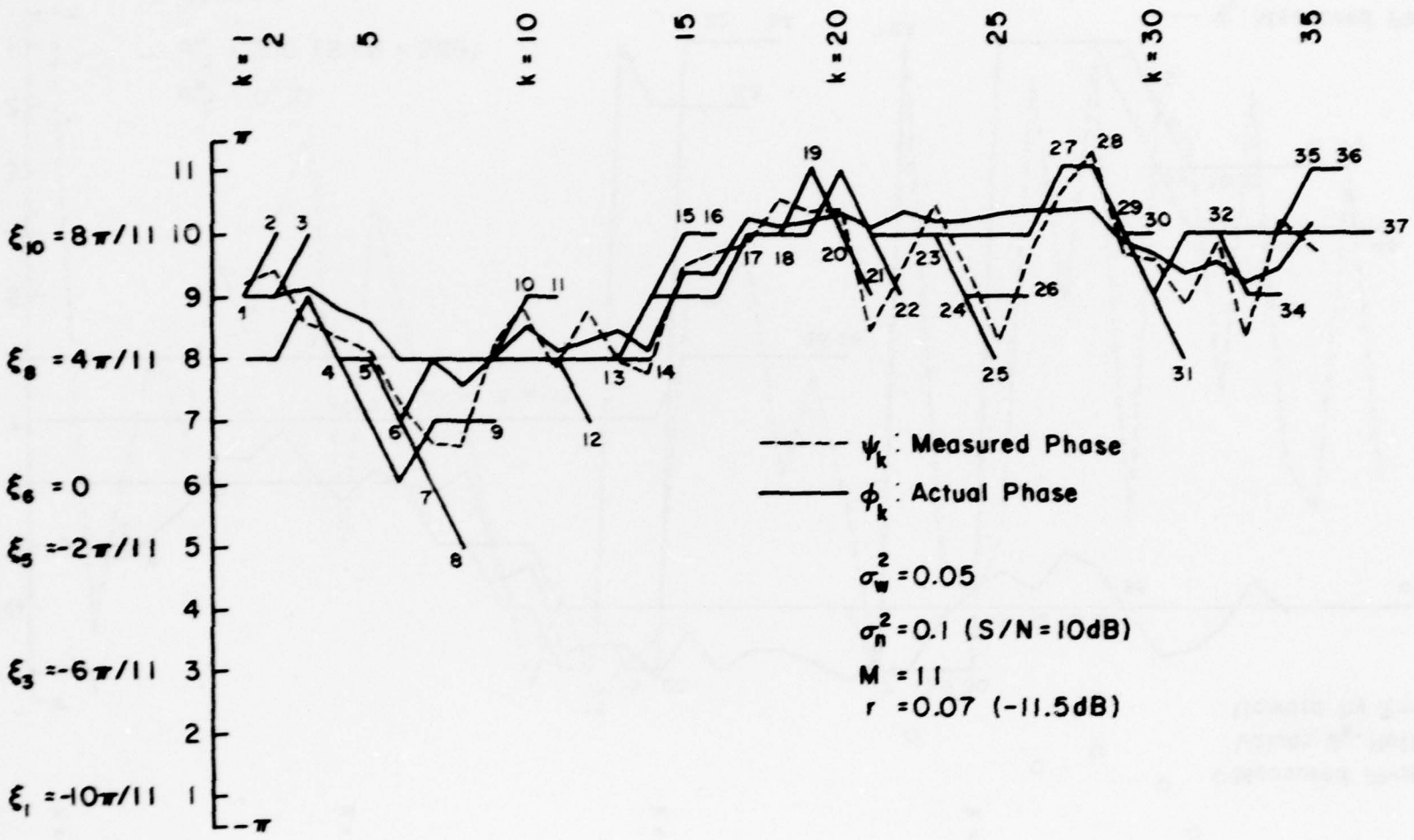

Figure 6. Typical Simulation: Decoding a MAP Phase Sequence

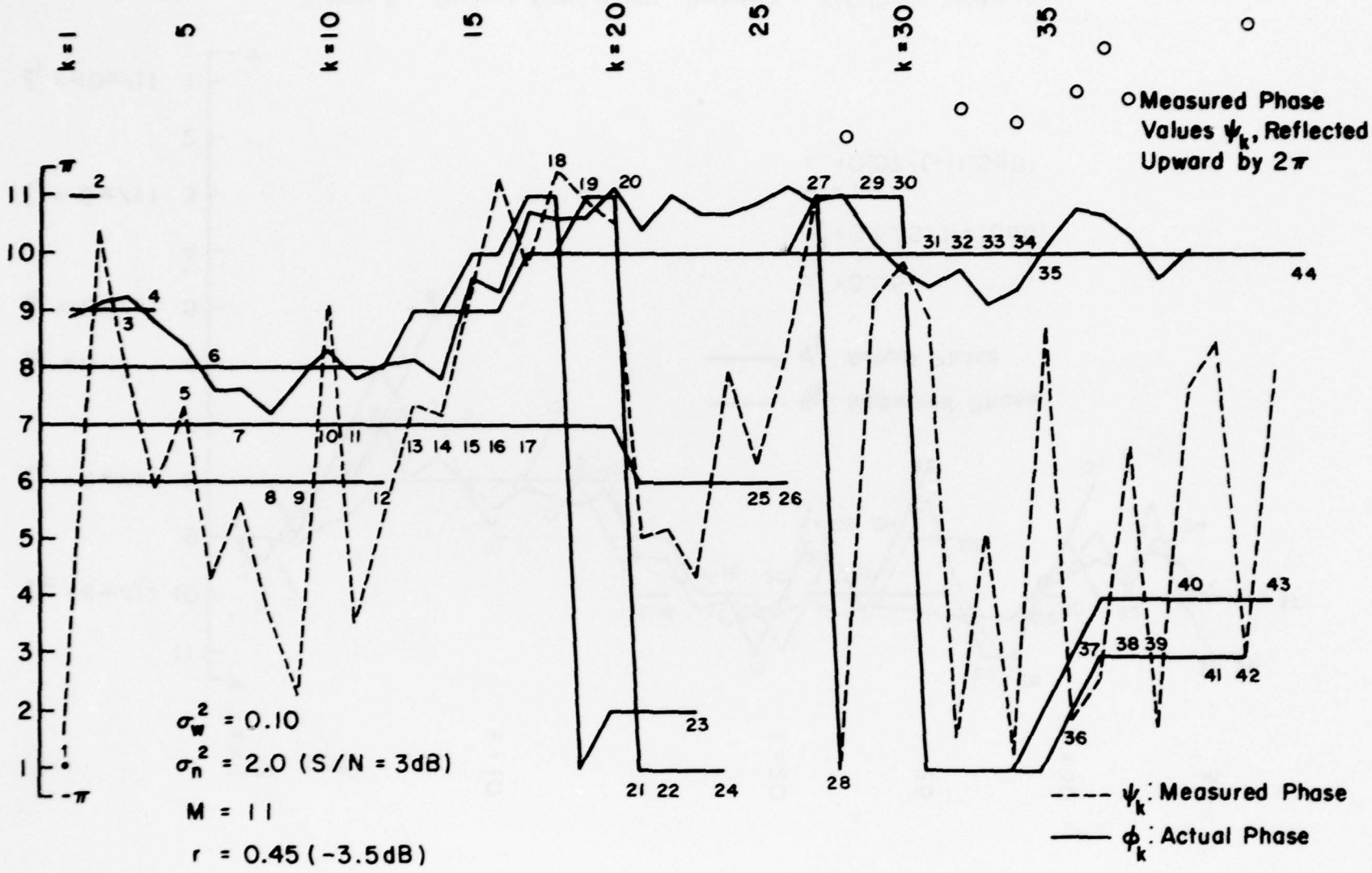

Figure 7. Typical Simulation: Decoding a Low S/N-High Variance Phase Sequence

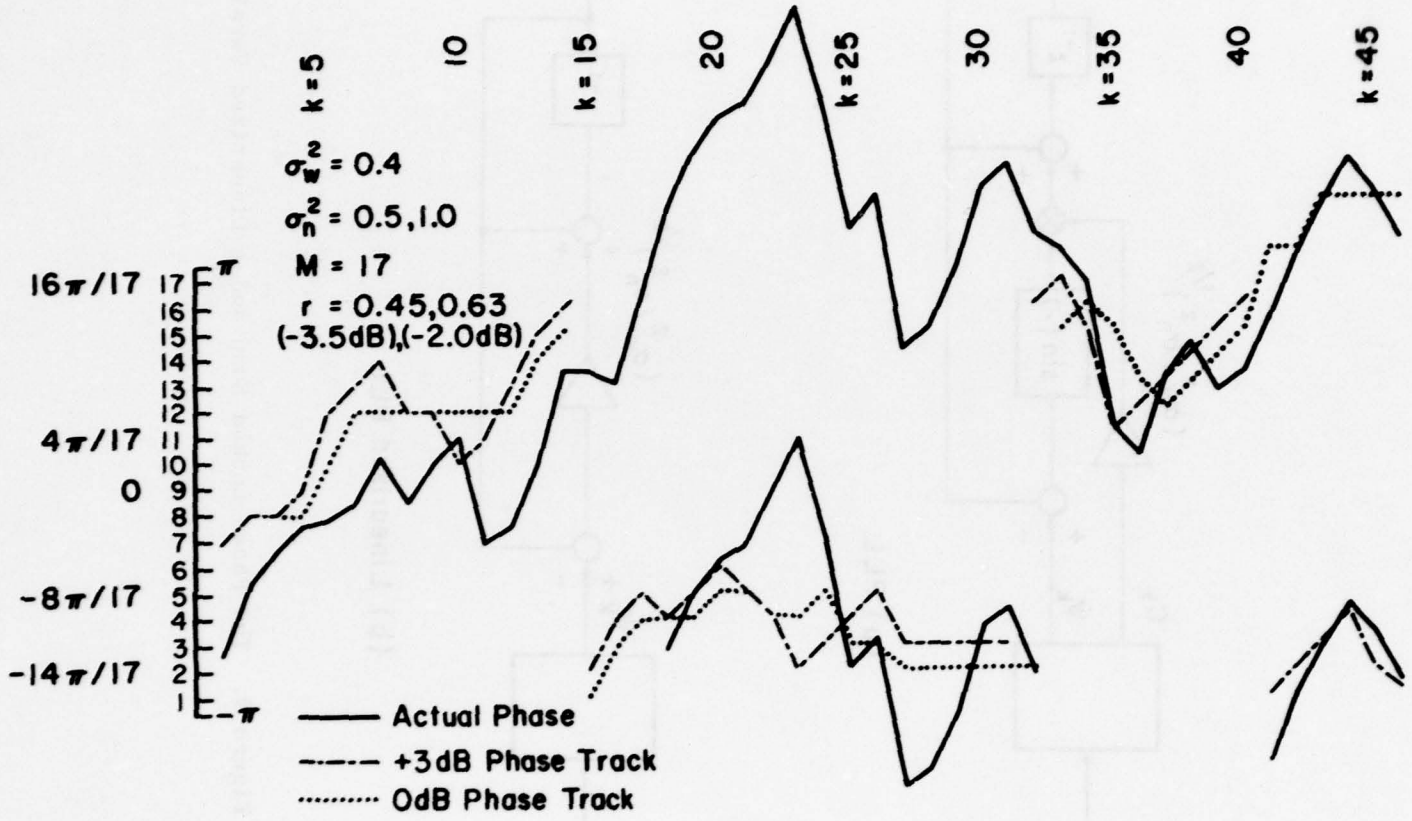

Figure 8. Typical Simulation: Decoding a Low S/N-Very High Variance Phase Sequence

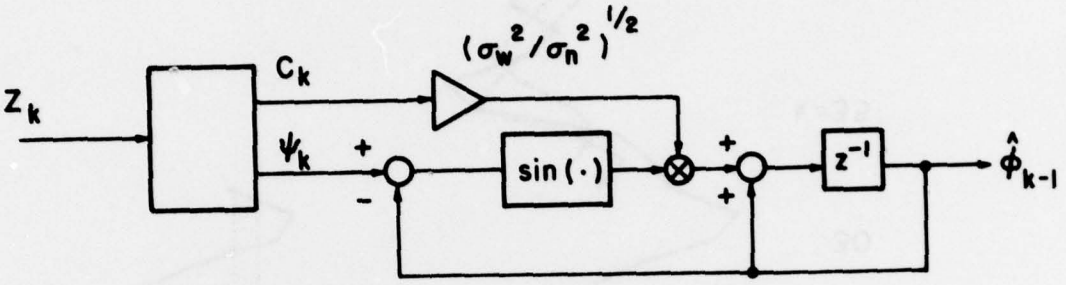

(a) PLL

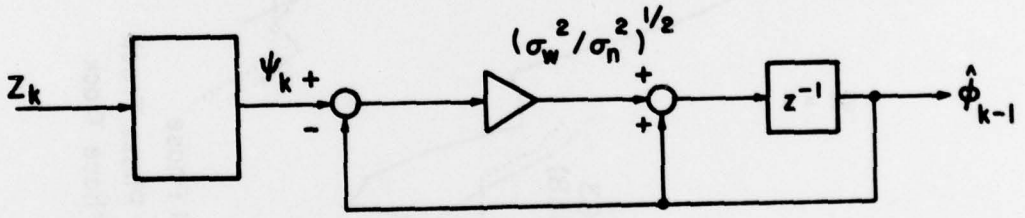

(b) Linearized PLL

Figure 9. The Phase Locked Loop and a Linearized Version

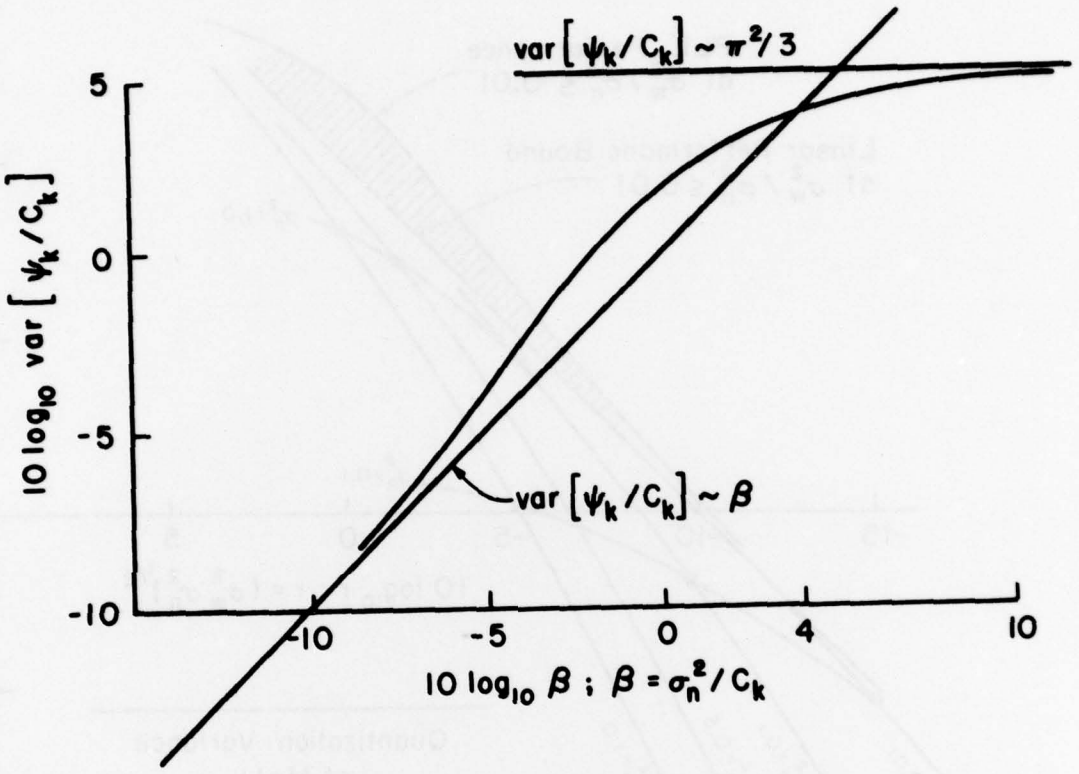

Figure 10. $\mathrm{Var}[\psi_k/C_k]$ vs. $\beta = \sigma_n^2/C_k$

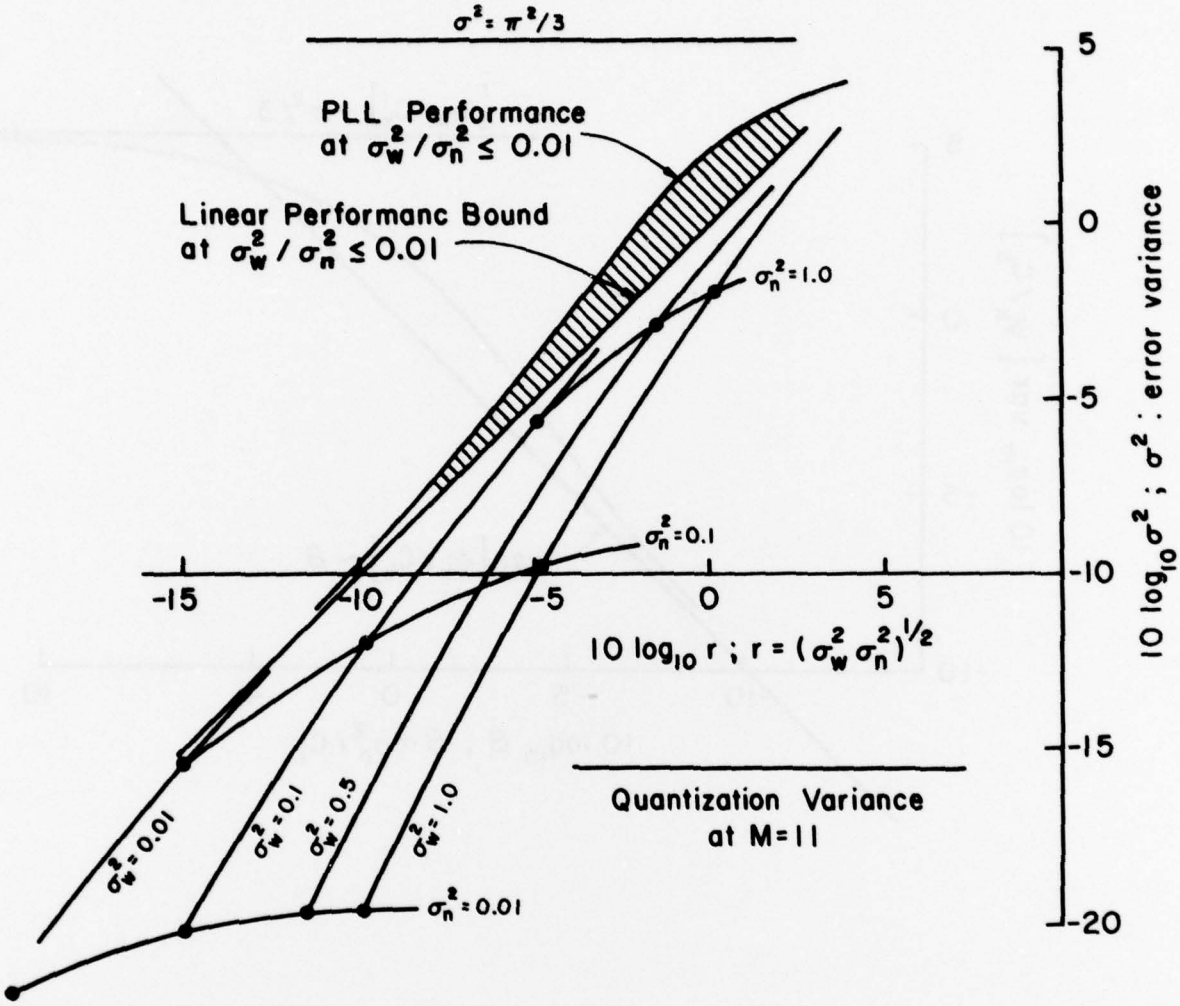

Figure 11. Performance Bounds

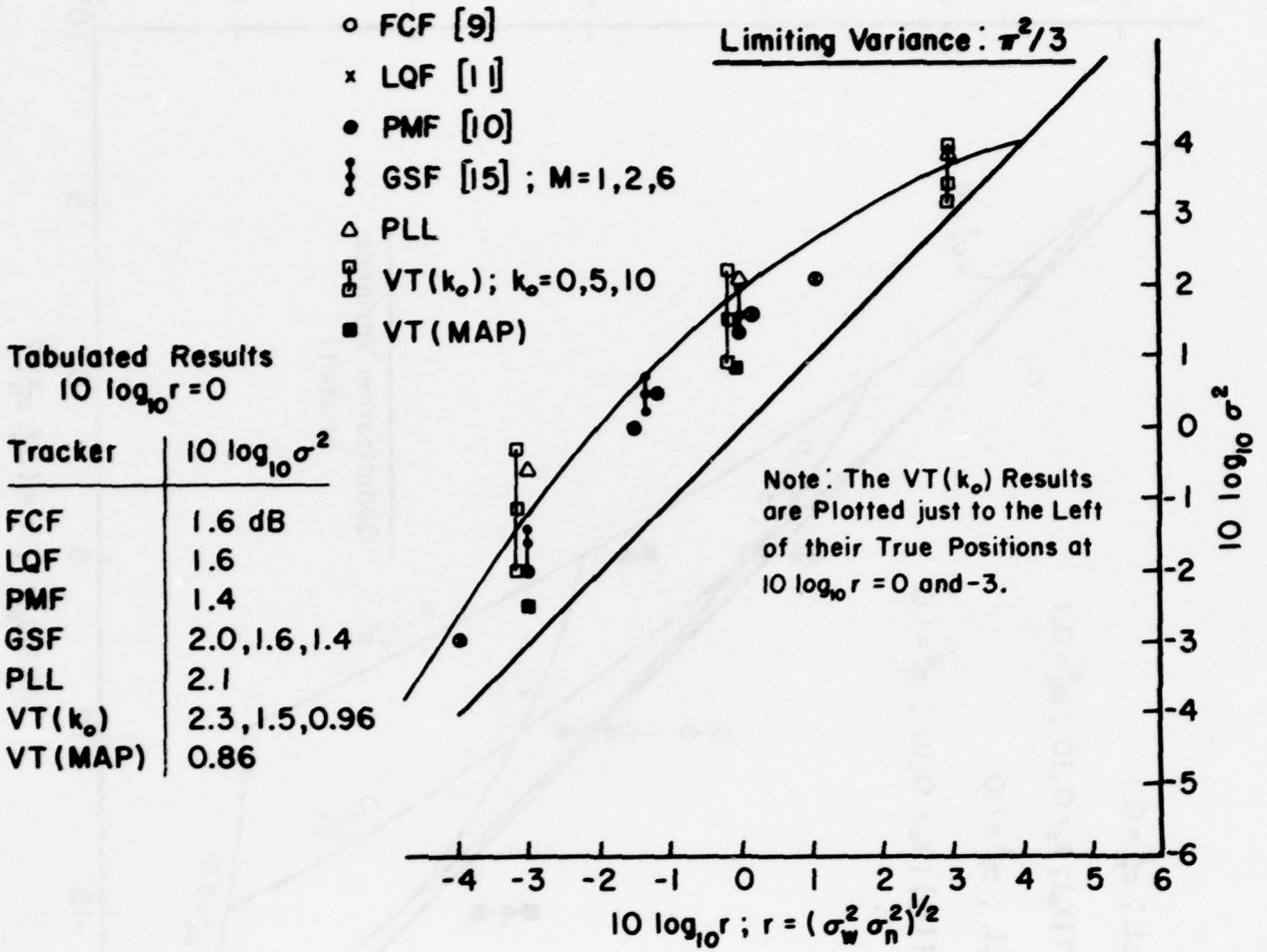

Tabulated Results
$10 \log_{10} r = 0$

Tracker	$10 \log_{10} \sigma^2$
FCF	1.6 dB
LQF	1.6
PMF	1.4
GSF	2.0, 1.6, 1.4
PLL	2.1
VT(k_o)	2.3, 1.5, 0.96
VT(MAP)	0.86

Figure 12. Performance Results for $\sigma_w^2/\sigma_n^2 = 0.01$

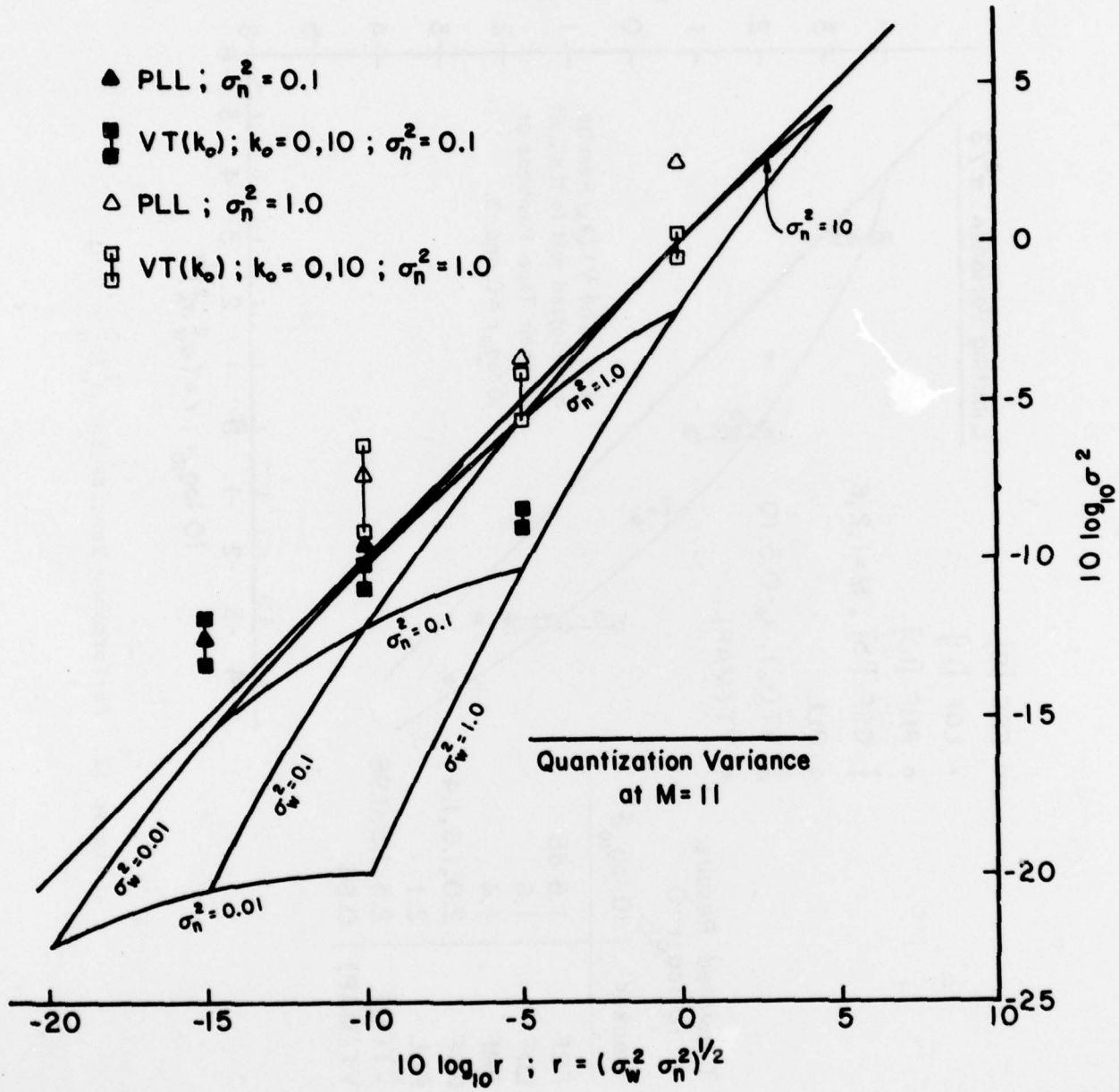

Figure 13. Performance Results for Various Values of σ_w^2/σ_n^2

σ_n^2	σ_w^2	σ_w^2/σ_n^2	$r=(\sigma_n^2\sigma_w^2)^{\frac{1}{2}}$	σ_{rad}^2 (dB)
10.0	0.01	0.001	0.316 (-5dB)	0.73 (-1.35dB)
10.0	0.10	0.01	1.0 (0dB)	1.25 (0.96dB)
10.0	1.0	0.1	3.16 (5dB)	2.32 (3.66dB)
1.0	0.01	0.01	0.10 (-10dB)	0.14 (-8.7dB)
1.0	0.10	0.10	0.316 (-5dB)	0.23 (-6.3dB)
1.0	1.0	1.0	1.0 (0dB)	0.90 (-0.45dB)
0.10	0.01	0.10	0.032 (-15dB)	0.048 (-13.2dB)
0.10	0.10	1.0	0.10 (-10dB)	0.079 (-11dB)
0.10	1.0	10.0	0.316 (-5dB)	0.124 (-9.1dB)
20.0	0.20	0.01	2.0 (3dB)	2.10 (3.24dB)
10.0	0.10	0.01	1.0 (0dB)	1.25 (0.96dB)
5.0	0.05	0.01	0.5 (-3dB)	0.63 (-1.99dB)

TABLE I. Performance Results for Viterbi Phase Tracker; $k_0 = 10$

Unclassified

SECURITY CLASSIFICATION OF THIS PAGE (When Data Entered)

REPORT DOCUMENTATION PAGE		READ INSTRUCTIONS BEFORE COMPLETING FORM
1. REPORT NUMBER Technical Report #27	2. GOVT ACCESSION NO.	3. RECIPIENT'S CATALOG NUMBER
4. TITLE (and Subtitle) Modulo-2π Phase Sequence Estimation		5. TYPE OF REPORT & PERIOD COVERED 6. PERFORMING ORG. REPORT NUMBER
7. AUTHOR(s) Louis L. Scharf Dennis D. Cox C. Johan Masreliez		8. CONTRACT OR GRANT NUMBER(s) N00014-75-C-0518
9. PERFORMING ORGANIZATION NAME AND ADDRESS Department of Electrical Engineering Colorado State University Fort Collins, CO 80523		10. PROGRAM ELEMENT, PROJECT, TASK AREA & WORK UNIT NUMBERS
11. CONTROLLING OFFICE NAME AND ADDRESS Office of Naval Research Statistics and Probability Branch Arlington, VA 22217		12. REPORT DATE FEBRUARY 1978 13. NUMBER OF PAGES 59
14. MONITORING AGENCY NAME & ADDRESS(if different from Controlling Office)		15. SECURITY CLASS. (of this report) Unclassified 15a. DECLASSIFICATION/DOWNGRADING SCHEDULE

16. DISTRIBUTION STATEMENT (of this Report)

Approved for public release; distribution unlimited.

17. DISTRIBUTION STATEMENT (of the abstract entered in Block 20, if different from Report)

18. SUPPLEMENTARY NOTES

19. KEY WORDS (Continue on reverse side if necessary and identify by block number)

MAP sequence estimation; nonlinear filtering, phase estimation, dynamic programming, Viterbi algorithm, estimation of random walk

20. ABSTRACT (Continue on reverse side if necessary and identify by block number)

The probabilistic evolution of random walk on the circle is studied and the results used to derive a MAP sequence estimator for phase. The sequence estimator is a Viterbi tracker for tracking phase on a finite-dimensional grid in $[-\pi,\pi)$. The algorithm is shown to provide a convenient method for obtaining fixed-lag phase sequence estimates. Performance characteristics are presented and compared with several other nonlinear filtering algorithms. The results indicate superior performance over the range of parameter values usually considered and excellent performance in parameter ranges corresponding to high

DD FORM 1 JAN 73 1473 EDITION OF 1 NOV 65 IS OBSOLETE
S/N 0102-014-6601

Unclassified

SECURITY CLASSIFICATION OF THIS PAGE (When Data Entered)

signal-to-noise ratio and rapidly fluctuating phase. Applications to coherent data communication systems are outlined.